AD NUMBER

ADB014346

NEW LIMITATION CHANGE

TO

Approved for public release, distribution unlimited

FROM

Distribution authorized to U.S. Gov't. agencies only; Test and Evaluation; OCT 1976. Other requests shall be referred to Air Force Armament Lab., Eglin AFB, FL 32542.

AUTHORITY

USADTC ltr, 2 Apr 1980

AEDC-TR-76-111
AFATL-TR-76-79

STATIC STABILITY CHARACTERISTICS OF THE MK-82/84 AIR-INFLATABLE RETARDER HIGH DRAG MODEL

PROPULSION WIND TUNNEL FACILITY
ARNOLD ENGINEERING DEVELOPMENT CENTER
AIR FORCE SYSTEMS COMMAND
ARNOLD AIR FORCE STATION, TENNESSEE 37389

October 1976

Final Report for Period 26 – 31 March 1976

Distribution limited to U.S. Government agencies only; this report contains information on test and evaluation of military hardware; October 1976; other requests for this document must be referred to Air Force Armament Laboratory (AFATL/DLJC), Eglin AFB, FL 32542.

Prepared for

AIR FORCE ARMAMENT LABORATORY (DLJC)
EGLIN AIR FORCE BASE, FLORIDA 32542

NOTICES

When U. S. Government drawings specifications, or other data are used for any purpose other than a definitely related Government procurement operation, the Government thereby incurs no responsibility nor any obligation whatsoever, and the fact that the Government may have formulated, furnished, or in any way supplied the said drawings, specifications, or other data, is not to be regarded by implication or otherwise, or in any manner licensing the holder or any other person or corporation, or conveying any rights or permission to manufacture, use, or sell any patented invention that may in any way be related thereto.

Qualified users may obtain copies of this report from the Defense Documentation Center.

References to named commercial products in this report are not to be considered in any sense as an endorsement of the product by the United States Air Force or the Government.

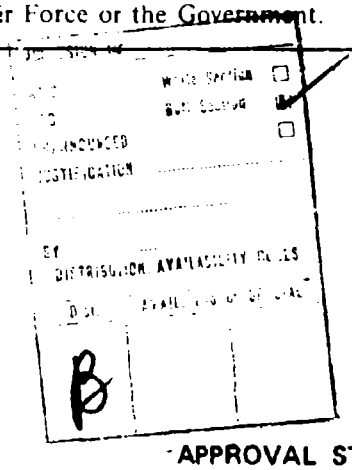

APPROVAL STATEMENT

This technical report has been reviewed and is approved for publication.

FOR THE COMMANDER

John C. Cardosi

JOHN C. CARDOSI
Lt Colonel, USAF
Chief Air Force Test Director, PWT
Directorate of Test

Alan L. Devereaux

ALAN L. DEVEREAUX
Colonel, USAF
Director of Test

UNCLASSIFIED

REPORT DOCUMENTATION PAGE	READ INSTRUCTIONS BEFORE COMPLETING FORM
1 REPORT NUMBER: AEDC-TR-76-111 / AFATL-TR-76-79 ✓	2 GOVT ACCESSION NO.	3 RECIPIENT'S CATALOG NUMBER
4 TITLE (and Subtitle): STATIC STABILITY CHARACTERISTICS OF THE MK-82/84 AIR-INFLATABLE RETARDER HIGH DRAG MODEL.	5 TYPE OF REPORT & PERIOD COVERED: Final Report, 26 - 31 March 1976
	6 PERFORMING ORG. REPORT NUMBER
7 AUTHOR(s): R. A. Paulk and C. F. Anderson, ARO, Inc.	8 CONTRACT OR GRANT NUMBER(s)
9 PERFORMING ORGANIZATION NAME AND ADDRESS: Arnold Engineering Development Center (XO), Air Force Systems Command, Arnold Air Force Station, TN 37389	10 PROGRAM ELEMENT, PROJECT, TASK AREA & WORK UNIT NUMBERS: Program Element 64[illegible]2F, Project 5713, Task 03
11 CONTROLLING OFFICE NAME AND ADDRESS: Air Force Armament Laboratory (AFATL/DLJC), Eglin Air Force Base, FL 32542	12 REPORT DATE: October 1976; 13 NUMBER OF PAGES: 64
14 MONITORING AGENCY NAME & ADDRESS (if different from Controlling Office): 12 66	15 SECURITY CLASS (of this report): UNCLASSIFIED; 15a DECLASSIFICATION DOWNGRADING SCHEDULE: N/A

16 DISTRIBUTION STATEMENT (of this Report)

Distribution limited to U.S. Covernment agencies only; this report contains information on test and evaluation of military hardware; October 1976; Other requests for this document must be referred to Air Force Armament Laboratory (AFATL/DLJC), Eglin AFB, FL 32542.

17 DISTRIBUTION STATEMENT (of the abstract entered in Block 20, if different from Report)

16 AF-5713, ARO-P41T-C7A; 17 5713Ø3

18 SUPPLEMENTARY NOTES

Available in DDC. 18 AFATL

19 TR-76-79

19 KEY WORDS (Continue on reverse side if necessary and identify by block number)

MK-82 bomb	ordnance
MK-84 bomb	parachutes
static stability	retarding
Ballutes	

20 ABSTRACT (Continue on reverse side if necessary and identify by block number)

An investigation was conducted in the Propulsion Wind Tunnel (16T) to obtain static stability characteristics of the MK-82 and MK-84 with air-inflatable Ballutes and selected fin configurations. The MK-82 model was 0.442 scale and had slotted fins with 12.5-deg spin wedges. The MK-84 model was 0.264 scale and had two sets of cambered fins. Each model was equipped with a fuse, lugs, and a lanyard pack. The tests were conducted for various model and Ballute roll orientations at Mach numbers from

DD FORM 1 JAN 73 1473 EDITION OF 1 NOV 65 IS OBSOLETE

UNCLASSIFIED

042550

20. ABSTRACT (Continued)

0.6 to 1.4 for angles of attack up to 20 deg and Reynolds numbers from 5.1×10^5 to 6.8×10^5 based on the centerbody maximum diameter. Model and Ballute roll orientation had only small effects on the normal-force, axial-force, and pitching-moment coefficients. Installing the Ballute with the Ballute inlets in the wake of the fins decreased the rolling-moment and yawing-moment coefficients and increased the side-force coefficient.

R

510,000 To 680,000

AFSC
Arnold AFS Tenn

PREFACE

The work reported herein was conducted by the Arnold Engineering Development Center (AEDC), Air Force Systems Command (AFSC), for the Air Force Armament Laboratory (AFATL/DLJC) under Program Element 64602F, Project 5713. The AFATL project monitor was Mr. Paul Shirey. The results of the test were obtained by ARO, Inc. (a subsidiary of Sverdrup & Parcel and Associates, Inc.), contract operator of AEDC, AFSC, Arnold Air Force Station, Tennessee. The work was done under ARO Project Number P41T-C7A. The authors of this report were R. A. Paulk and C. F. Anderson, ARO, Inc. The data analysis was completed on April 29, 1976, and the manuscript (ARO Control No. ARO-PWT-TR-76-63) was submitted for publication cn June 16, 1976.

CONTENTS

ILLUSTRATIONS

1.0 INTRODUCTION

An investigation to determine the six-component static-stability coefficients of the MK-82 and MK-84 bombs with fabric Ballutes® [air-inflatable retarders (AIR)] was conducted in the Propulsion Wind Tunnel (16T), Propulsion Wind Tunnel Facility (PWT). The bombs were tested with selected fin configurations and at various Ballute and tail roll orientations. Data were obtained at Mach numbers from 0.6 to 1.4 at a constant total pressure of 800 psfa. The Reynolds number range, based on center-body maximum diameter, was from 5.1×10^5 to 6.8×10^5.

2.0 APPARATUS

2.1 TEST FACILITY

Tunnel 16T is a closed circuit, continuous flow, variable density wind tunnel capable of operating at Mach numbers between 0.2 and 1.6. The tunnel is equipped with a plenum evacuation system, and the test section is formed by fixed, parallel top and bottom perforated walls, and perforated variable angle side walls. The test section is 16 by 16 ft in cross section and 40 ft long. (A more complete description of the wind tunnel, its operating characteristics, and support equipment is given in Ref. 1.) The location of the test model and the model support system in the test area is indicated in Fig. 1, and photographs of the model installations are shown in Fig. 2.

2.2 TEST ARTICLES

2.2.1 MK-82 Bomb Model

Details of the MK-82 test model are shown in Fig. 3. The MK-82 bomb configuration was 0.442 scale and represented the MK-82 warhead and the BSU-49/B stabilizer assembly. The model had a fuse, lugs, lanyard pack, latch, and spring housing. The stabilizer assembly was fitted with four slotted fins equipped with 12.5-deg spin wedges. There were additional fin mounting holes to provide for testing with the fins in the (+) or (x) positions. The lanyard pack, latch, and spring housings

were similarly rotated; however, the lugs remained in the vertical plane. A "whisker"-type boundary-layer trip was located near MS 1.0. The boundary-layer trip was attached to the forebody and consisted of two rows of 0.007-in.-diam copper wires located approximately 0.1 in. apart, protruding approximately one wire diameter. The wires in the second row were staggered relative to the wires in the first row.

2.2.2 MK-84 Bomb Model

Details of the MK-84 test model are shown in Fig. 4. The MK-84 bomb configuration was 0.264 scale and represented the MK-84 warhead and the BSU-50/B stabilizer assembly. The model had a fuse, lugs, and lanyard pack.

Two fin configurations, differing in both span and airfoil shape, were used during the test of the MK-84. The fins were cambered to produce a positive static rolling moment. The entire afterbody of the model had to be rotated for testing at different fin roll orientations. The lugs, however, remained in the vertical plane.

The MK-84 and MK-82 had the same forebody, and, therefore, the same "whisker" boundary-layer trip.

2.2.3 Ballute (AIR)

Details of the Ballutes are shown in Fig. 5. The Ballute was a ram-air inflatable spheroid and was attached directly to the model base. In this application it was primarily a decelerator, but it provided some pitch and yaw stabilization as well. In operational use, the Ballute would be contained within the afterbody prior to deployment. However, for these tests the Ballutes were already deployed.

The Ballutes tested were made of fabric and were scale models of the full-size Ballutes, except that no closure plate was attached to the models. Each Ballute was pear shaped, with four scoop inlets and a toroidal

burble fence near its equator. The Ballute attachment to model bases allowed for rotation relative to the model base.

2.3 INSTRUMENTATION

Model forces and moments were measured with a six-component, internal strain-gage balance. The model angle of attack was measured with the pitch sector angle-of-attack indicator and was corrected for sting and balance deflections resulting from aerodynamic forces and moments on the model. Electrical signals from the balance and tunnel instrumentation were processed by the PWT data acquisition system and digital computer for online data reduction. Balance outputs were also recorded on an electrostatic recorder for monitoring model dynamic oscillati

3.0 TEST DESCRIPTION

3.1 TEST PROCEDURES AND CONDITIONS

Static force and moment data for the MK-82 and MK-84 stores with inflated Ballutes were obtained for Mach numbers from 0.6 to 1.4 for an angle-of-attack range from 0 to 20 deg. MK-82 data were obtained with the fins in the (x) orientation and the Ballute at roll angles of 0 and -45 deg. The lugs were in the vertical plane and were on the windward side as the model was pitched.

MK-84 data were obtained with the fins in the (+) and (x) orientation and the Ballute at a roll angle of -45 deg. The lugs were in the vertical plane and were on the windward side as the model was pitched.

The total pressure was held at 800 psfa, and the variation of Reynolds number and dynamic pressure with Mach number is shown in Fig. 6.

The data were reduced to coefficient form in the aeroballistic axis system with the moment reference at MS 15.416 for the MK-82 model and at MS 13.166 for the MK-84 model. The axis system and sign convention are presented in Fig. 7.

3.2 PRECISION OF MEASUREMENTS

3.2.1 Test Conditions

The uncertainties in angle of attack and roll angle are ±0.06 deg and ±0.10 deg, respectively. The estimated uncertainties in the tunnel Mach number and tunnel dynamic pressure are given in the following table and are based on a 95-percent probability.

	Mach Number						
	0.6	0.8	0.9	1.0	1.1	1.2	1.4
ΔM_∞	0.002	0.003	0.004	0.005	0.007	0.008	0.012
Δq_∞	1.230	1.930	2.540	3.200	3.960	4.680	5.700

3.2.2 Aerodynamic Coefficients

The estimated uncertainties in the aerodynamic coefficients for the MK-82 and MK-84 bombs are given in the following tables are based on a 95-percent probability.

MK-82

	Mach Number					
	0.6	0.8	0.9	1.0	1.1	1.2
ΔC_N	0.184	0.125	0.115	0.114	0.124	0.123
ΔC_Y	0.149	0.101	0.089	0.081	0.075	0.071
ΔC_A	0.252	0.173	0.179	0.223	0.267	0.257
ΔC_ℓ	0.072	0.048	0.042	0.039	0.036	0.034
ΔC_m	0.242	0.173	0.200	0.257	0.332	0.331
ΔC_n	0.186	0.126	0.110	0.101	0.093	0.089

MK-84
Mach Number

	0.6	0.8	0.9	1.0	1.1	1.2	1.4
ΔC_N	0.183	0.123	0.109	0.102	0.097	0.094	0.083
ΔC_Y	0.150	0.100	0.089	0.080	0.075	0.071	0.068
ΔC_A	0.243	0.165	0.149	0.141	0.139	0.134	0.112
ΔC_ℓ	0.071	0.048	0.042	0.038	0.036	0.034	0.033
ΔC_m	0.230	0.155	0.141	0.137	0.136	0.131	0.105
ΔC_n	0.187	0.125	0.110	0.100	0.093	0.089	0.085

4.0 RESULTS

4.1 MK-82 BOMB

The effects of Ballute roll orientation on the static stability characteristics of the MK-82 model at -45 deg roll are shown in Fig. 8 for all Mach numbers of interest. Normal-force and pitching-moment coefficients had slightly larger absolute values for the $\phi_B = 0$ configuration than for the $\phi_B = -45$ deg configuration. The axial-force coefficients were nearly equal for both Ballute roll orientations for subsonic Mach numbers. For $M_\infty = 1.1$ the $\phi_B = 0$ configuration had a higher axial-force coefficient.

The fin spin wedges generated a positive rolling moment on the MK-82 model, as is shown in Ref. 2. Adding the Ballute produced a negative model rolling-moment coefficient for both Ballute roll orientations for $M_\infty = 0.6$. For higher Mach numbers, only the $\phi_B = -45$ deg configuration (Ballute inlets in line with fins) produced a negative model rolling-moment coefficient.

The side-force coefficient generally tended to decrease with increasing angle of attack while the yawing-moment coefficient increased. Both side-force and yawing-moment coefficients generally showed a break or change in slope at $\alpha = 9$ deg. The reason for this change in slope is

not readily apparent; however, it should be noted that the Ballute stayed approximately aligned with the airflow as angle of attack increased. Therefore, the changes observed at α = 9 deg could have been produced by the Ballute's moving into the vortices being shed by the forebody. Rolling the Ballute to ϕ_B = -45 deg (inlets aligned with the fins) generally reversed the side-force and yawing-moment coefficients.

4.2 MK-84 BOMB

The MK-84 was tested with the ballute at -45 deg roll orientation for all test conditions. The effects of fin roll orientation on the static stability characteristics of the MK-84 with T2 fins are shown in Fig. 9. The configuration with the fins in the (+) orientation had the largest absolute values of normal-force and pitching-moment coefficient. The axial-force coefficient was largest for the model with (+) fin orientation for M_∞ = 0.6, 0.8, and 0.9. For M_∞ = 1.1, the axial-force coefficients were nearly equal for both fin orientations. When the Ballute inlets were aligned with the fins (ϕ_M = -45 deg), the rolling-moment coefficient was either reduced or negative.

The side-force coefficient generally tended to decrease with increasing angle of attack, whereas the yawing-moment coefficient increased, as was the case for the MK-82. The side-force coefficient was generally larger and the yawing-moment coefficient was generally smaller for the case with the fins and Ballute inlets aligned, ϕ_M = -45 deg.

The effect of fin size and camber on the static stability characteristics of the MK-84 store is shown in Fig. 10. For α < 6 deg, the T3 fins produced slightly larger absolute values of normal-force and pitching-moment coefficients than the T2 fins. For higher angles of attack, the two sets of fins produced nearly equal normal-force and pitching-moment coefficients. The axial-force coefficients were nearly the same for both configurations.

The T3 fins produced a larger side-force coefficient and a smaller yawing-moment coefficient than did the T2 fins. The T3 fins produced a larger rolling-moment coefficient than did the T2 fins.

REFERENCES

1. Test Facilities Handbook (Tenth Edition). "Propulsion Wind Tunnel Facility, Vol. 4." Arnold Engineering Development Center, May 1974.

2. Anderson, C. F. and Carleton, W. E. "Static and Dynamic Stability Characteristics of the Fixed-Fin and Inflatable Stabilizer Retarder Configurations of the MK-82 Store at Transonic Speeds." AEDC-TR-75-149 (AD-B007733L), November 1975.

blank
12

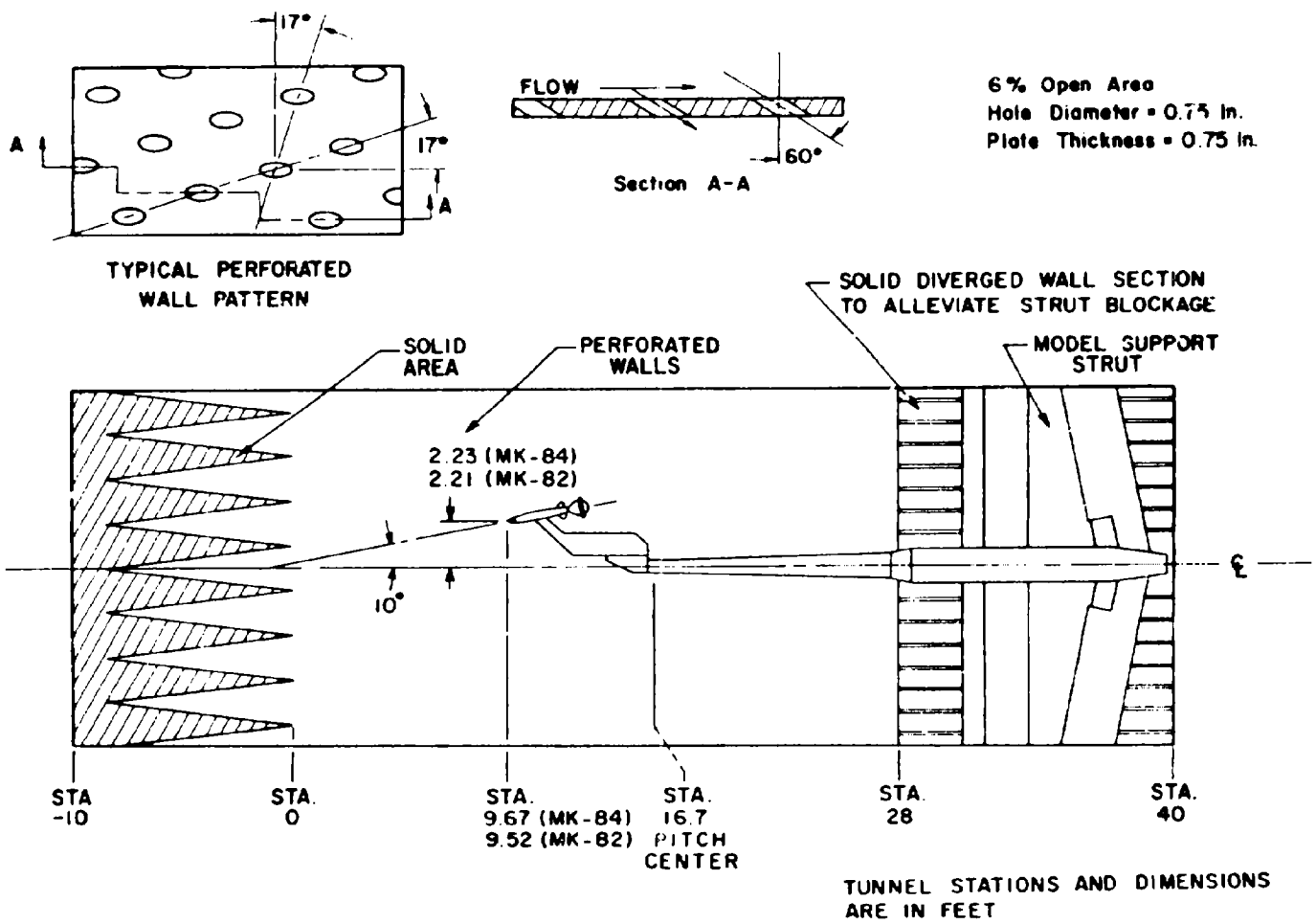

Figure 1. Schematic of model installation.

AEDC TR 76-111

a. MK-82

Figure 2. Photographs of model installation.

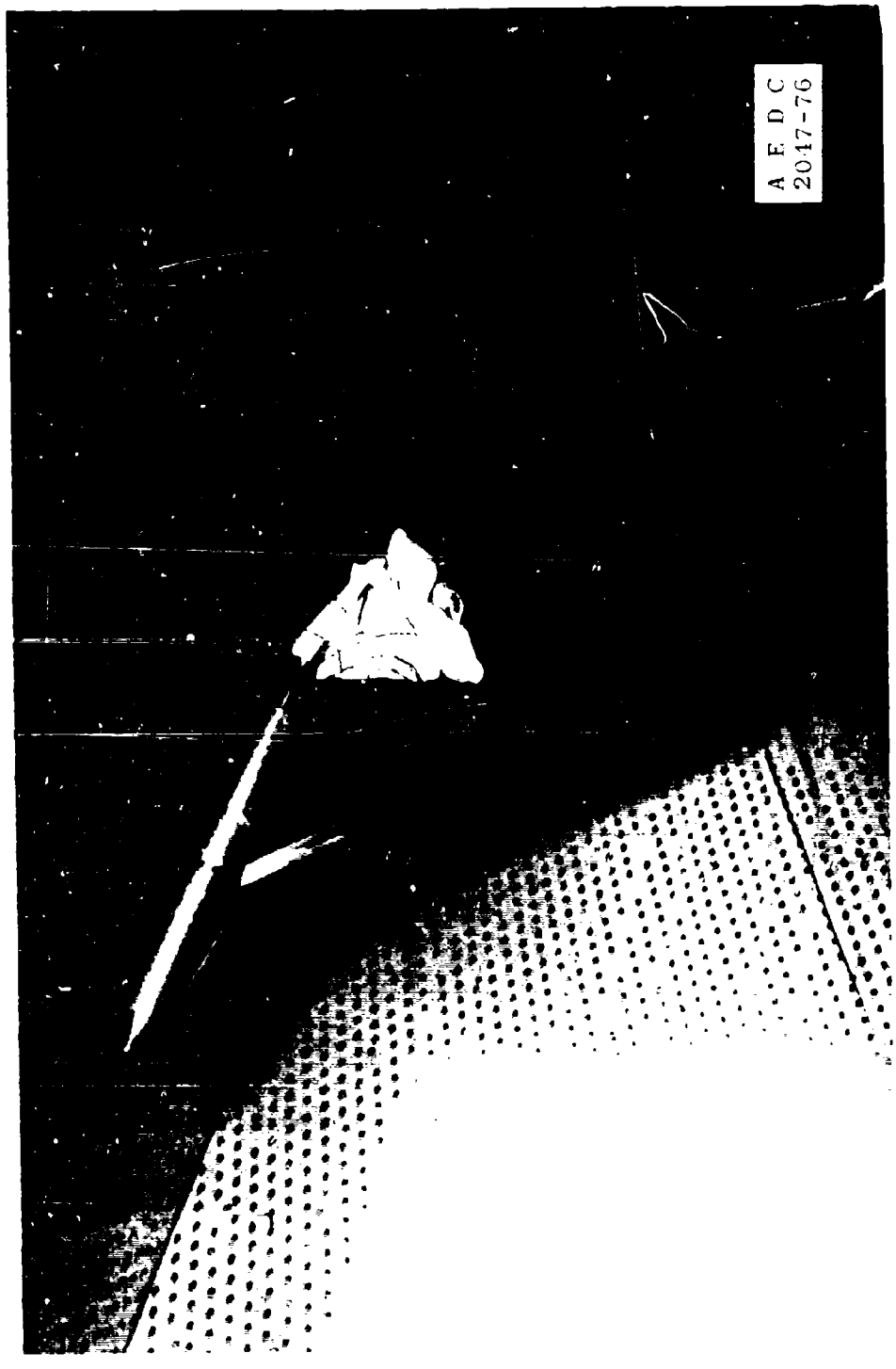

b. MK-84

Figure 2. Concluded.

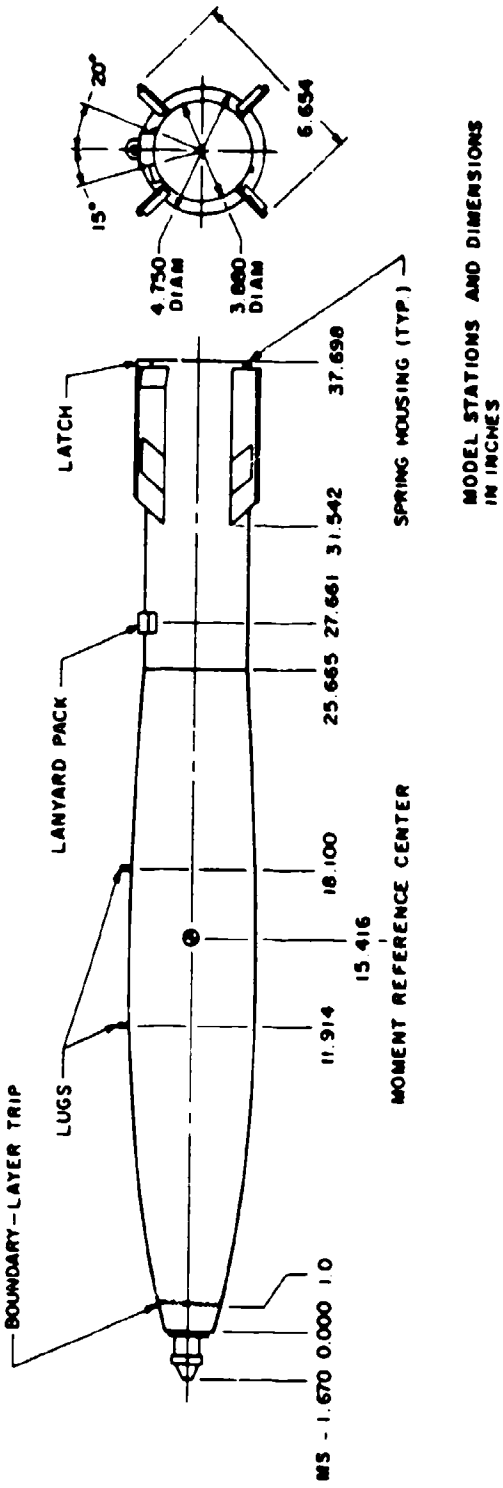

a. Model dimensions and fin orientation

Figure 3. MK-82 model details.

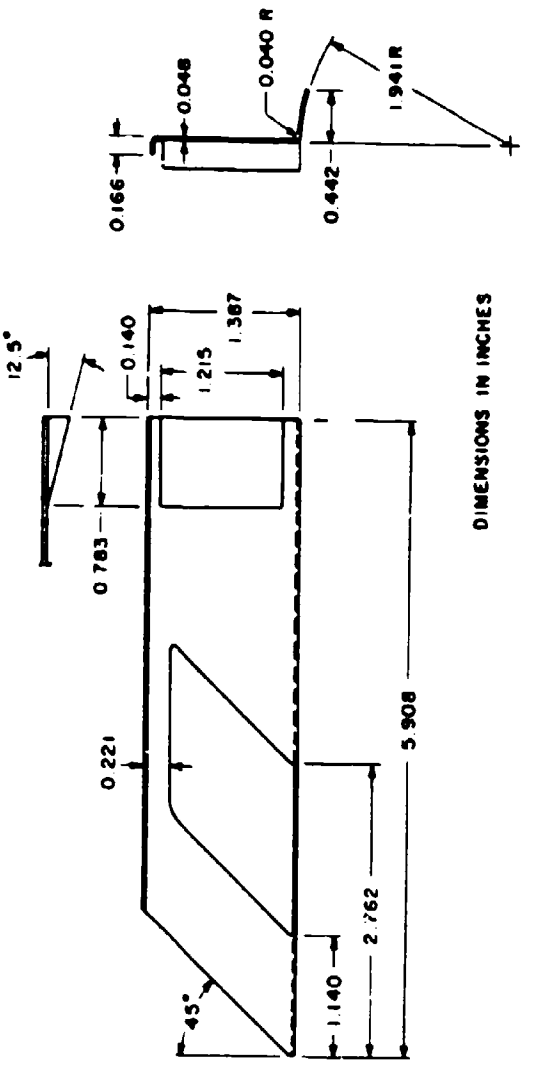

b. Fin dimensions
Figure 3. Continued.

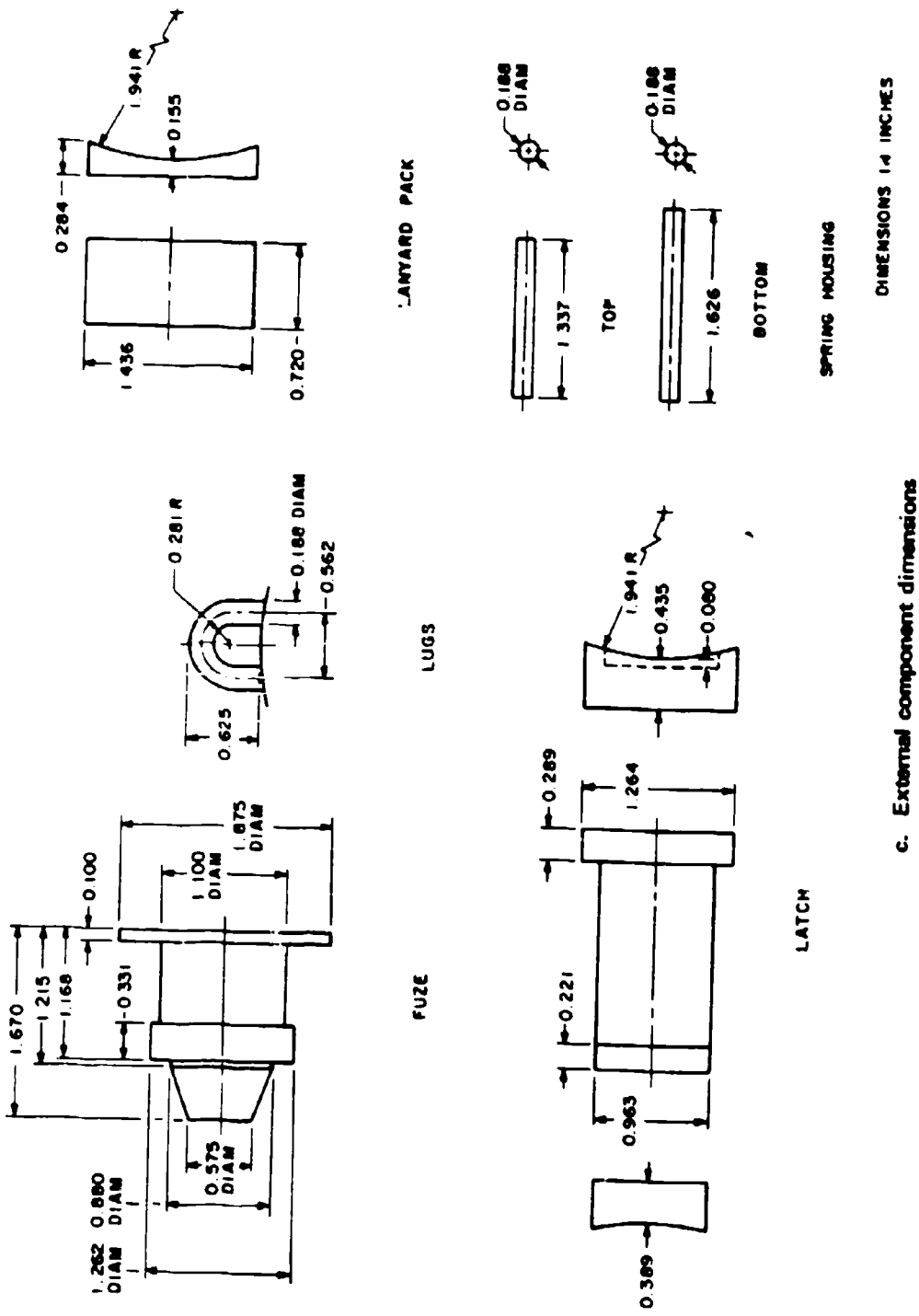

c. External component dimensions
Figure 3. Concluded.

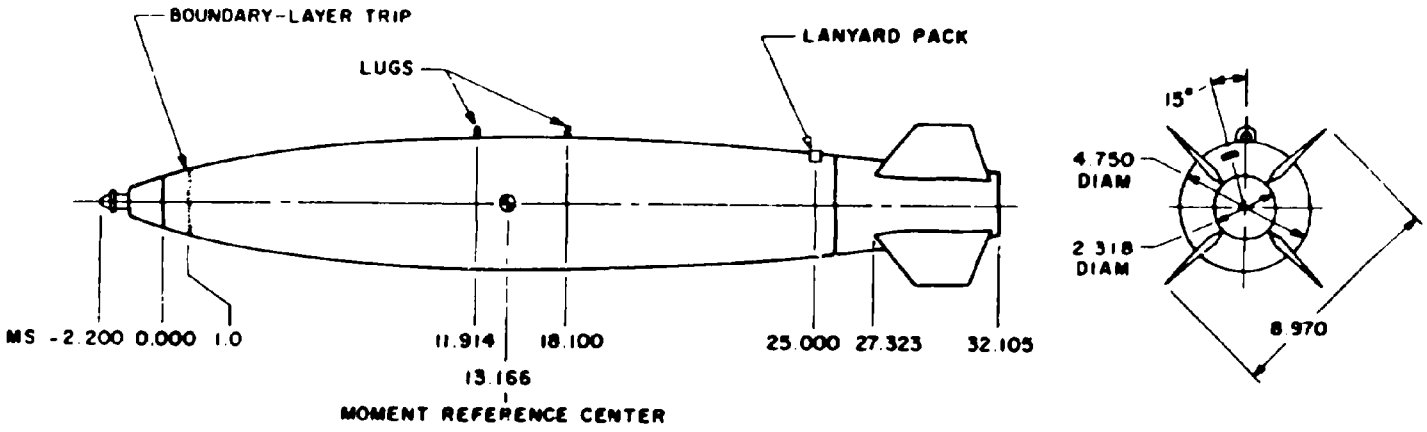

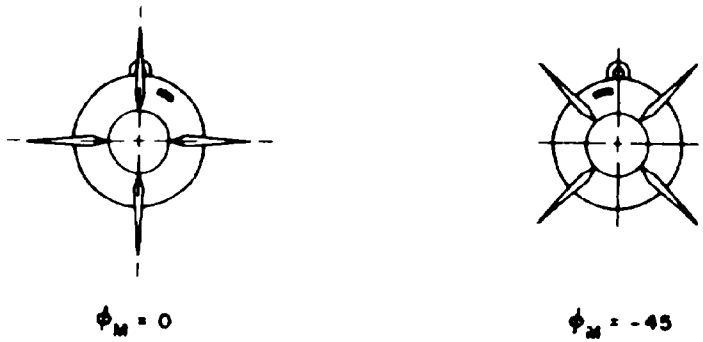

a. Model dimensions and fin orientation

Figure 4. MK-84 model details.

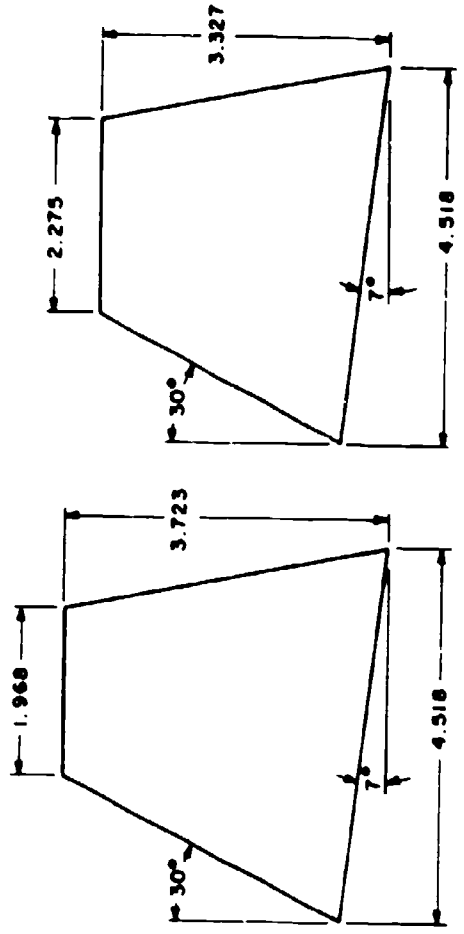

b. Fin dimensions and identification
Figure 4. Continued.

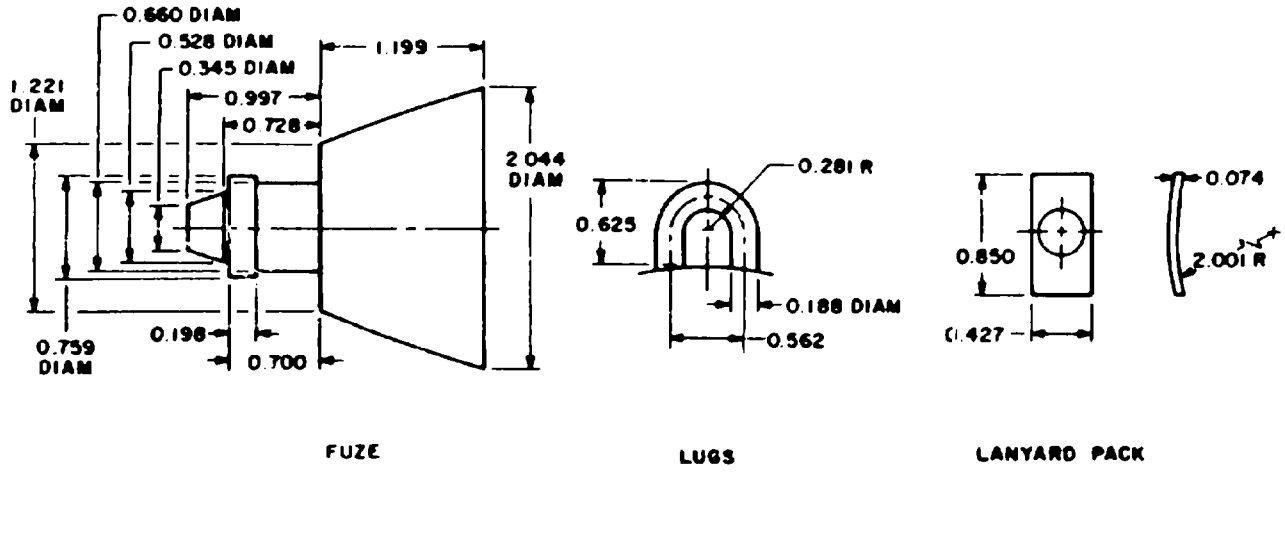

c. External component dimensions
Figure 4. Concluded.

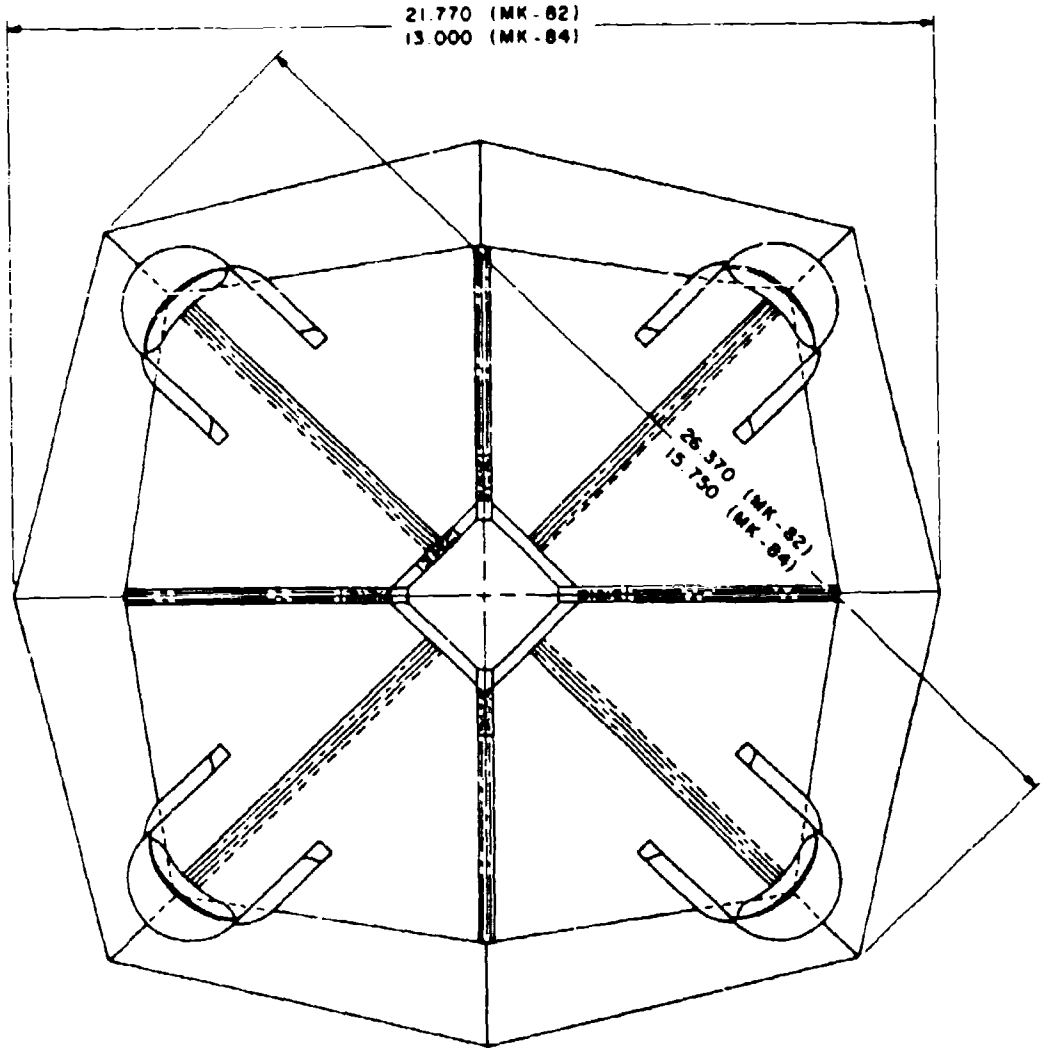

a. Front view showing ballute dimensions and roll orientation

Figure 5. Ballute details.

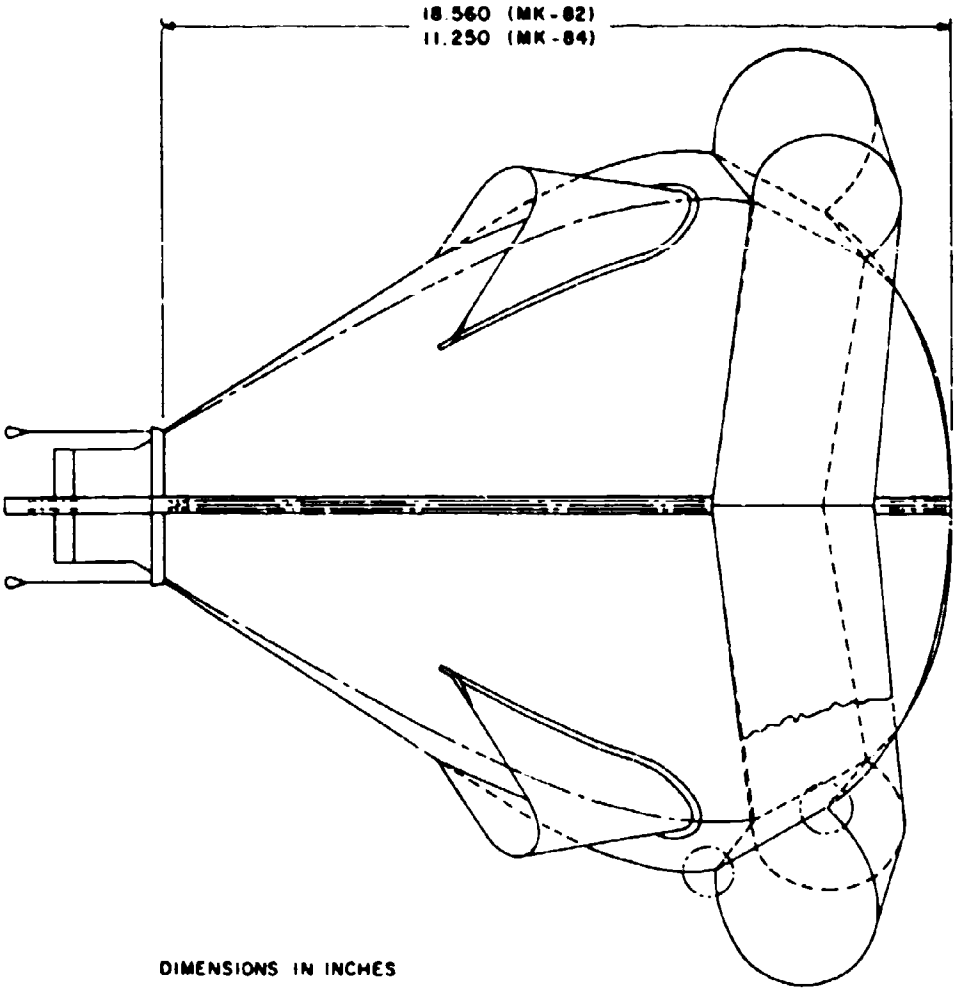

b. Side view showing ballute dimensions
Figure 5. Concluded.

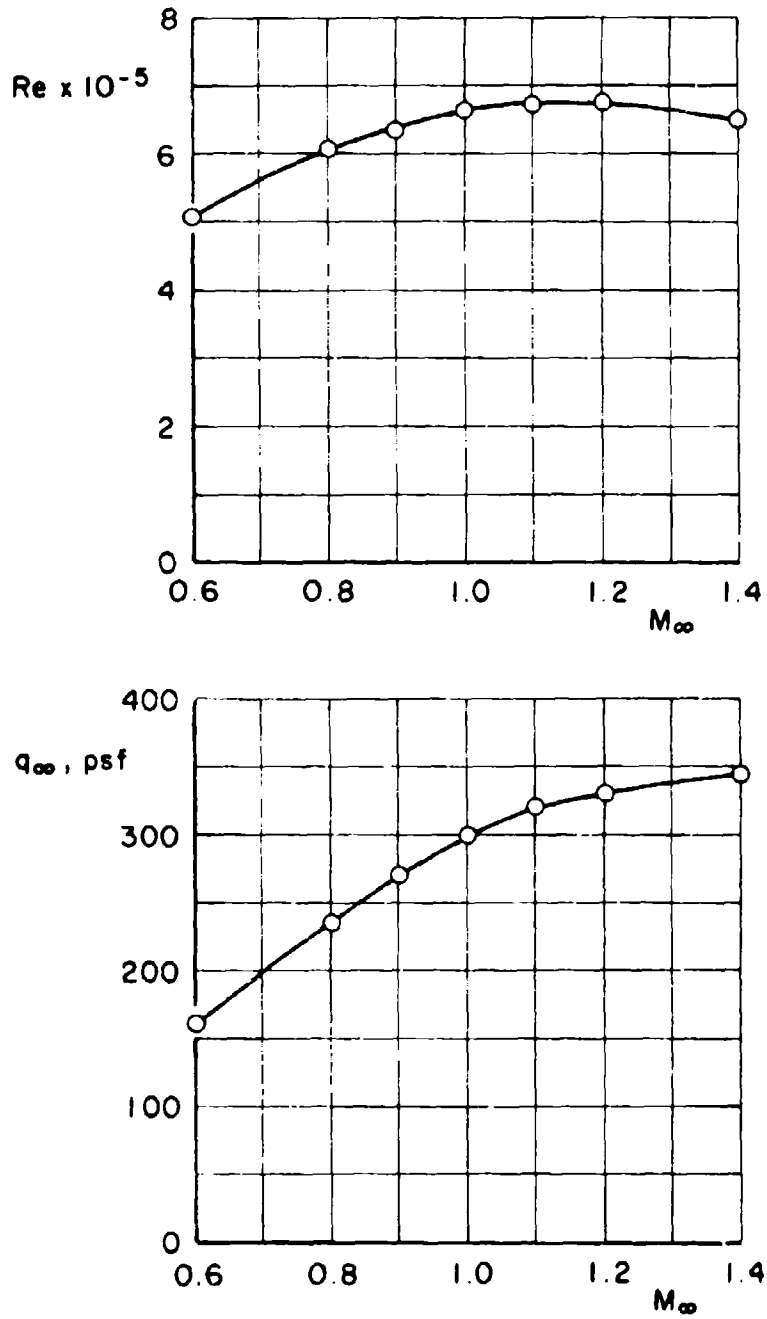

Figure 6. Variation of Reynolds number and dynamic pressure with Mach number.

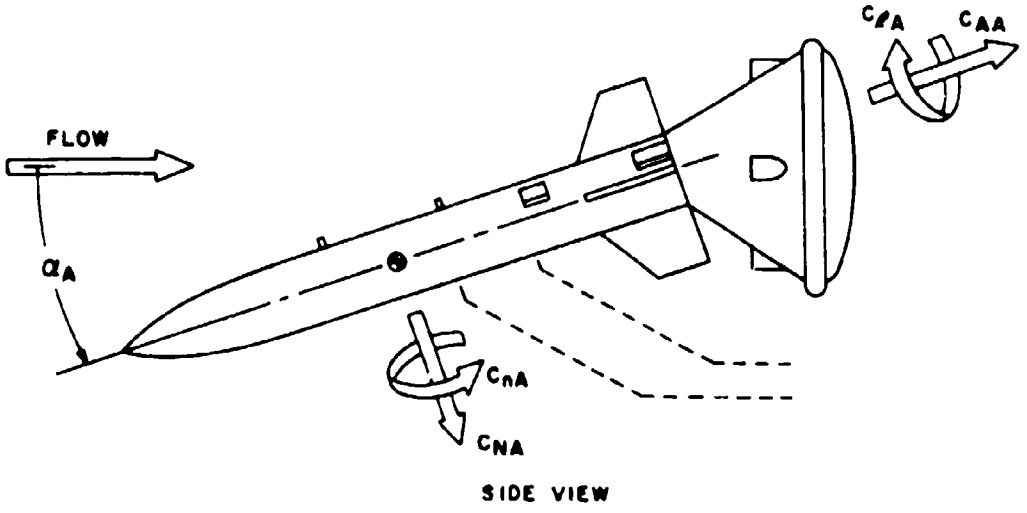

ARROWS INDICATE POSITIVE DIRECTION
OF FORCES, MOMENTS AND ANGLES

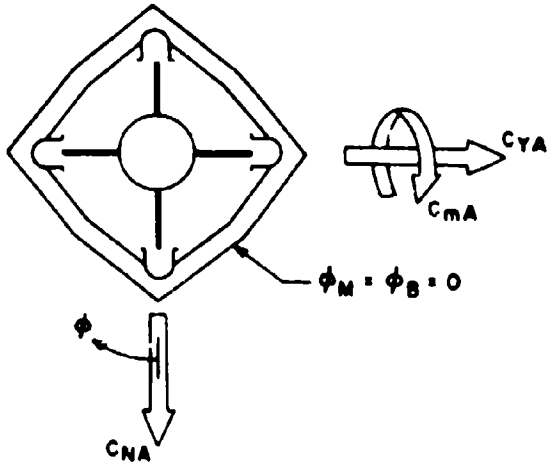

Figure 7. Axis system and sign convention.

SYM	M_∞	ϕ_B
⊙	0.6	0
⊡	0.6	-45

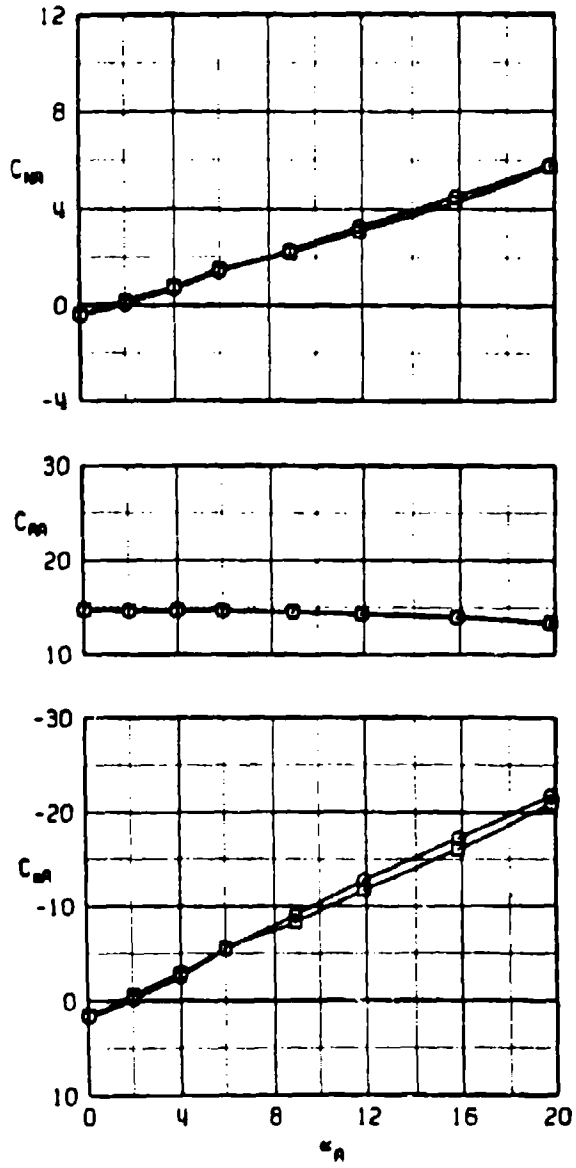

a. $M_\infty = 0.6$

Figure 8. Effects of ballute roll orientation on the static stability characteristics of the MK-82, ϕ_M = -45 deg.

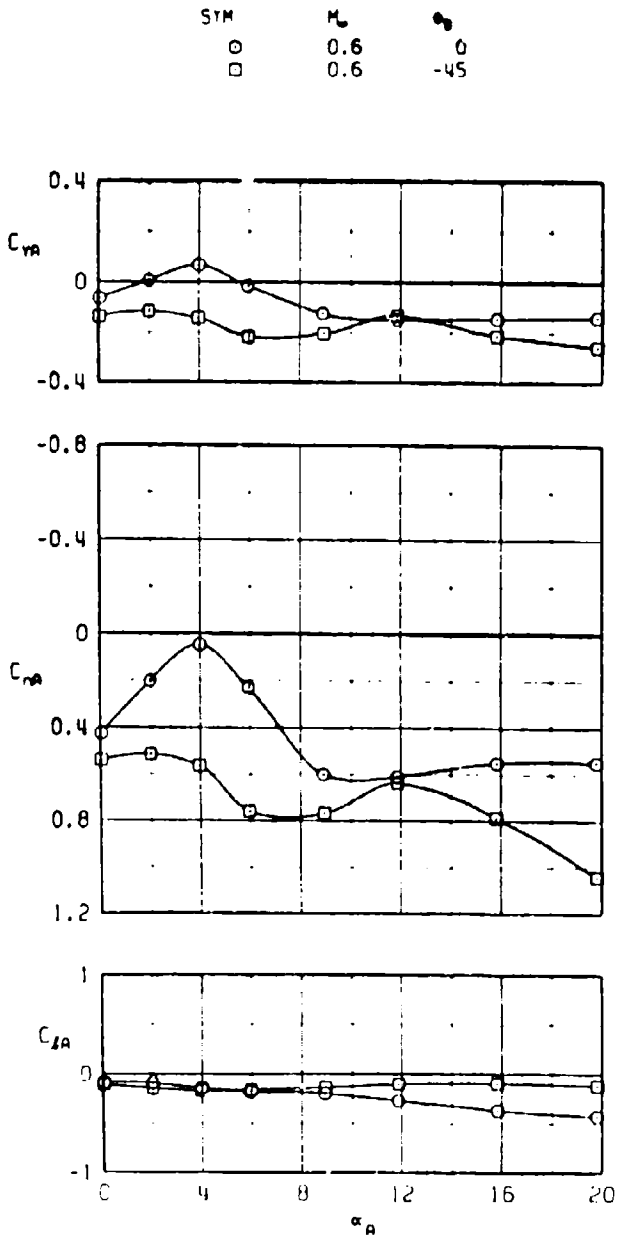

a. Concluded
Figure 8. Continued.

SYM	M_∞	ϕ_b
○	0.8	0
□	0.8	-45

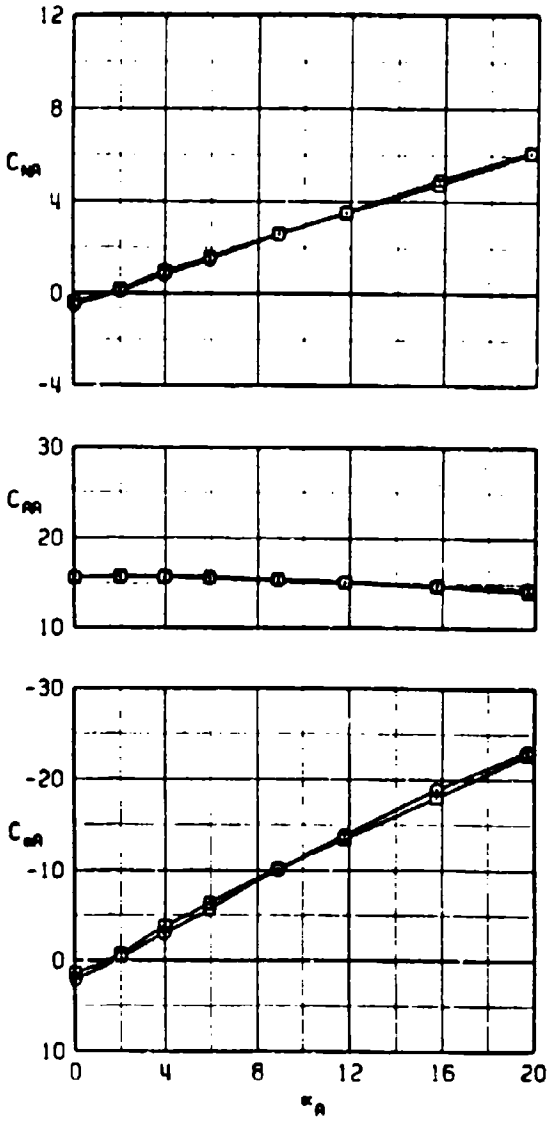

b. M_∞ = 0.8
Figure 8. Continued.

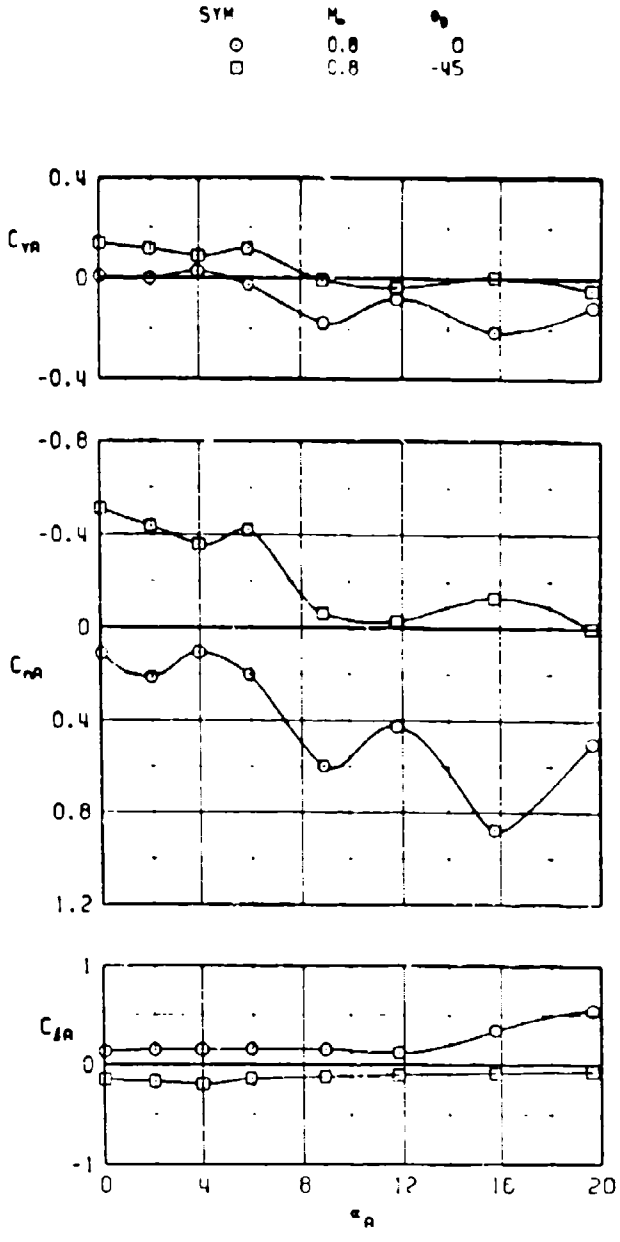

b. Concluded
Figure 8. Continued.

SYM	M_∞	ϕ_b
⊙	0.9	0
⊡	0.9	-45

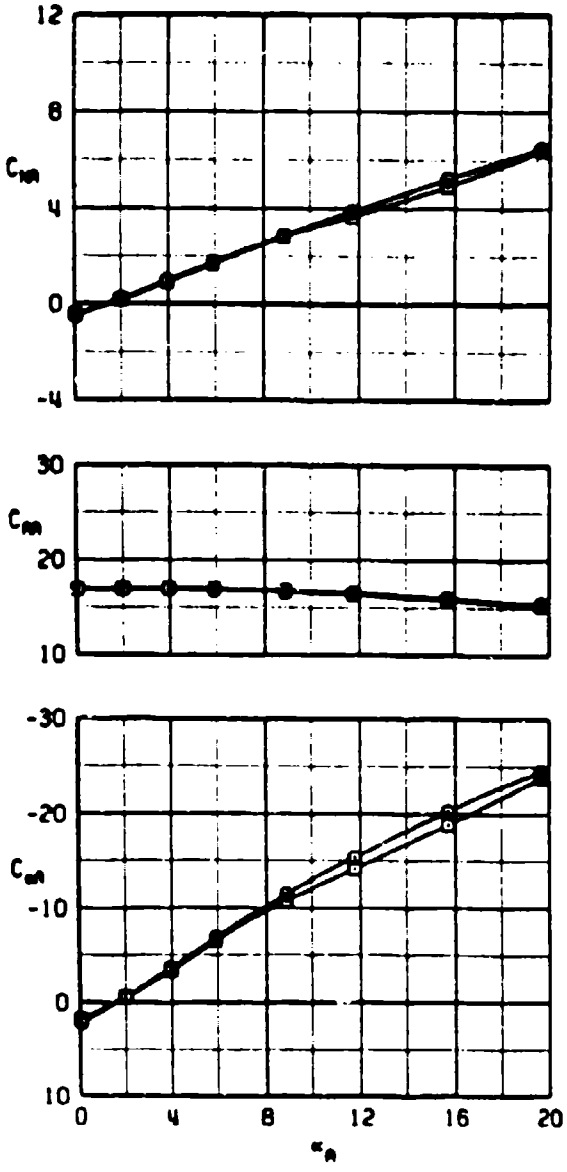

c. $M_\infty = 0.9$

Figure 8. Continued.

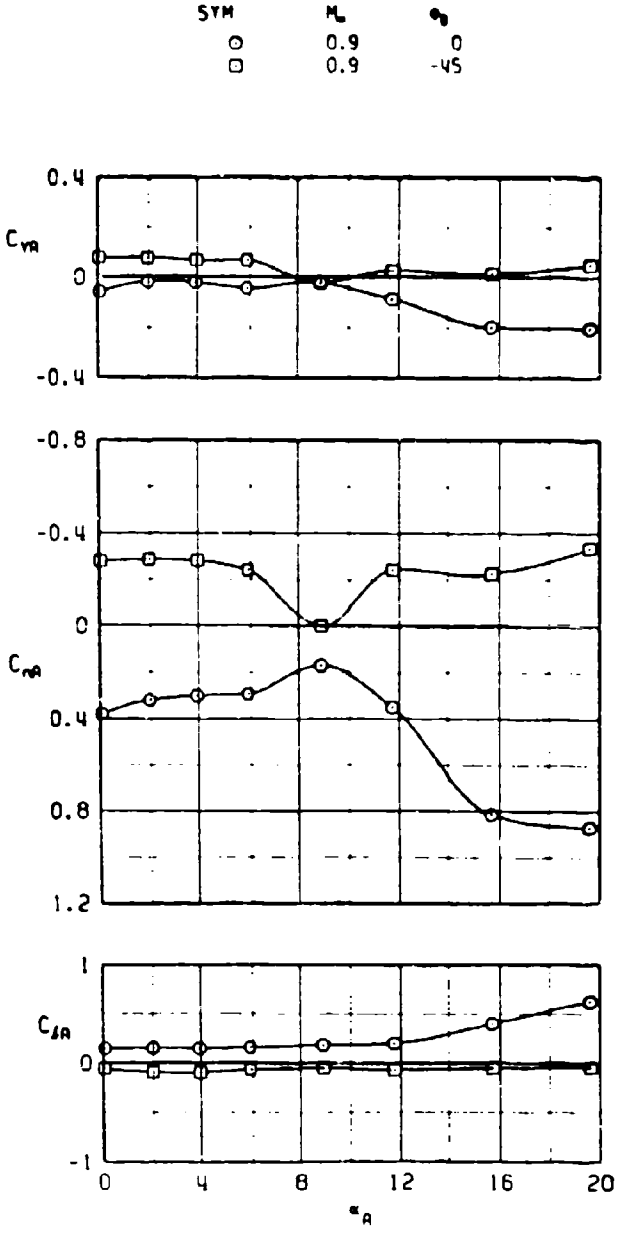

c. Concluded
Figure 8. Continued.

SYM	M_∞	ϕ_p
⊡	1.0	-45

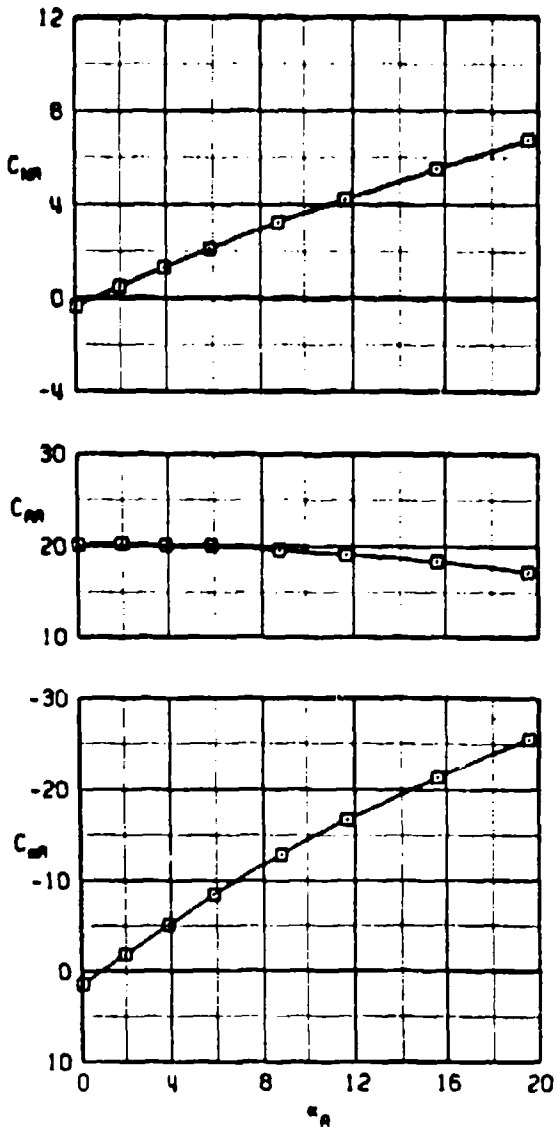

d. M_∞ = 1.0
Figure 8. Continued.

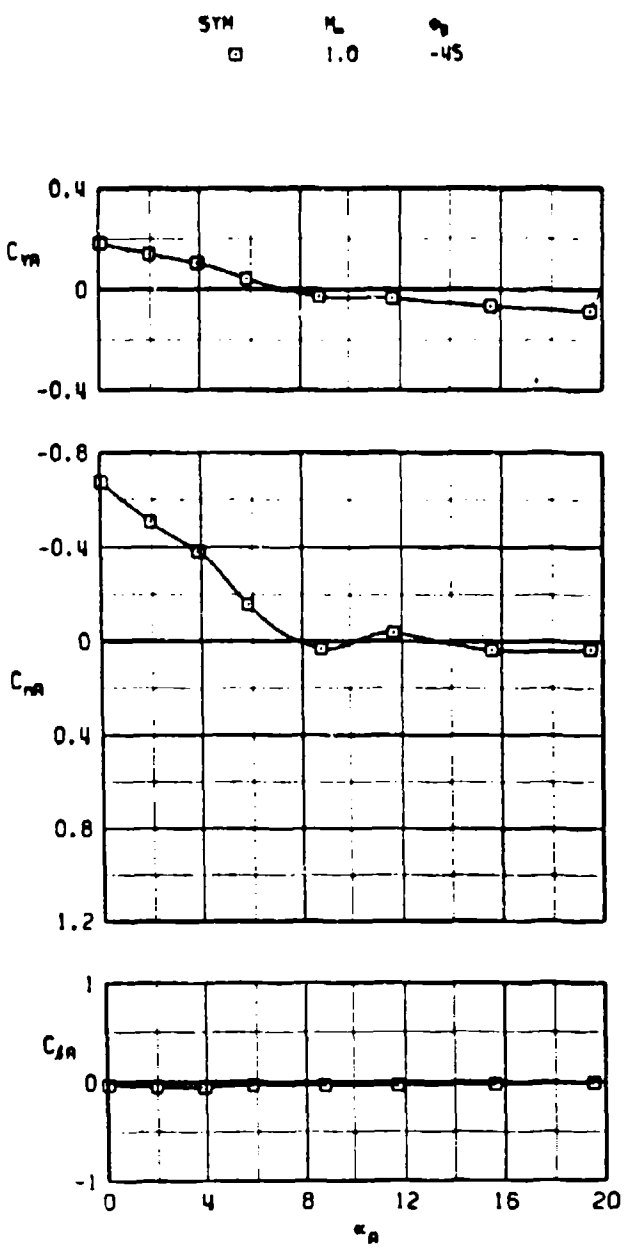

d. Concluded
Figure 8. Continued.

SYM	M_∞	ϕ_B
○	1.1	0
□	1.1	-45

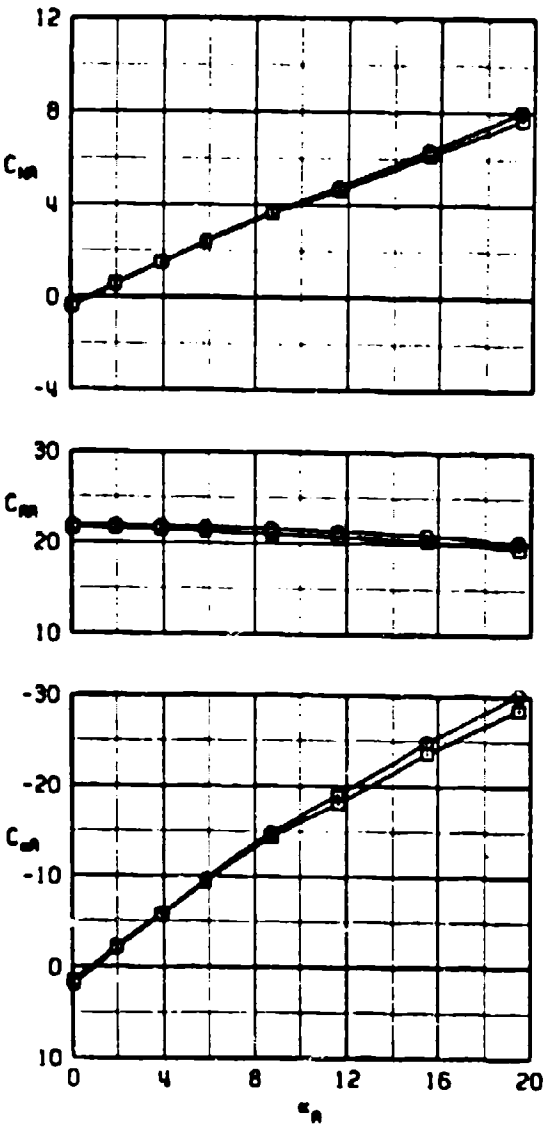

a. M_∞ = 1.1
Figure 8. Continued.

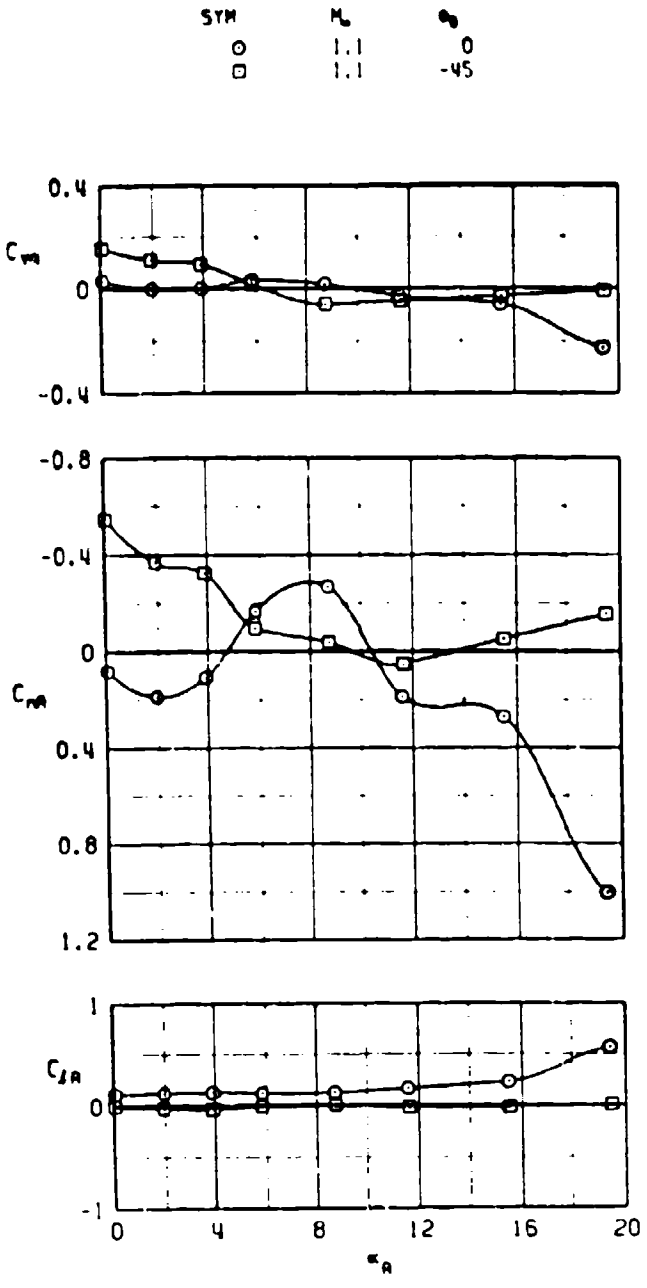

e. Concluded
Figure 8. Continued.

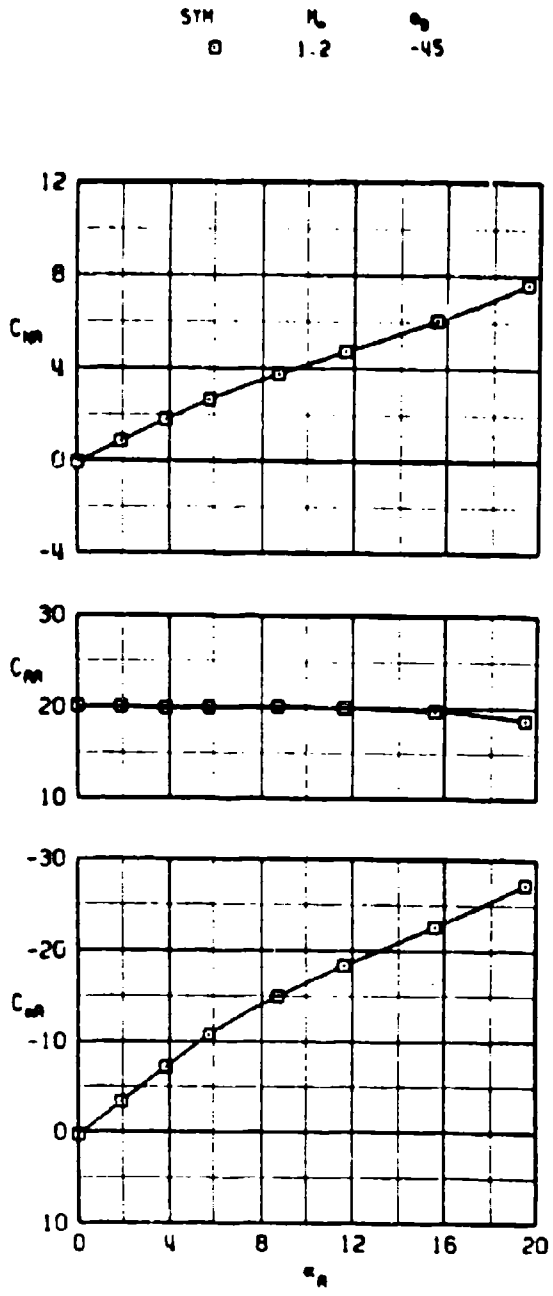

f. $M_\infty = 1.2$

Figure 8. Continued.

SYM	M_∞	ϕ_B
□	1.2	-45

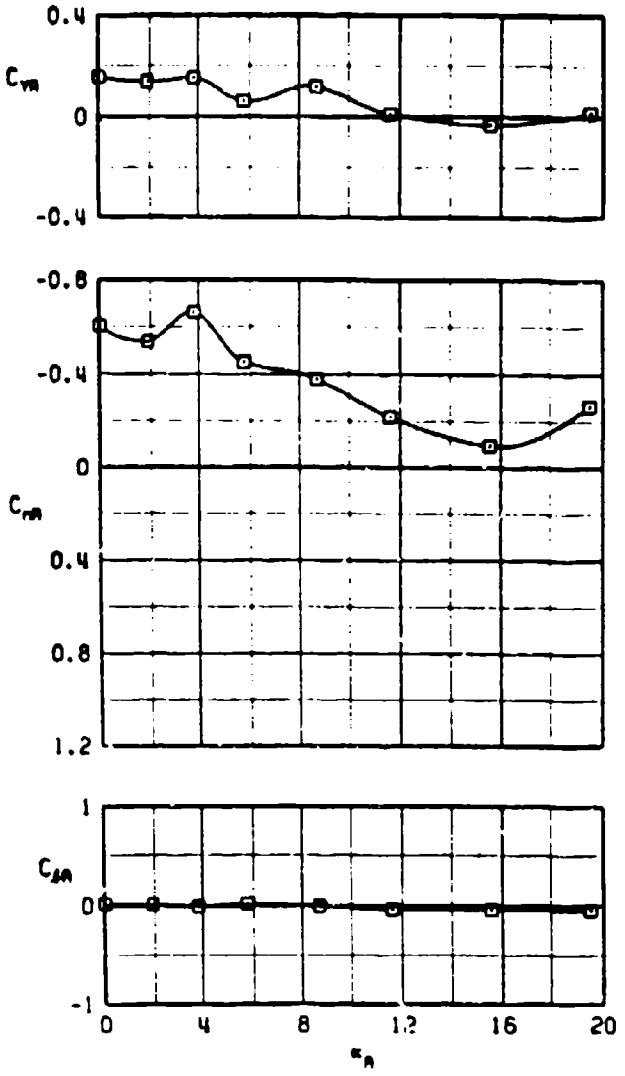

f. Concluded
Figure 8. Concluded.

SYMBOL	M_∞	ϕ_B
⊙	0.6	0
□	0.6	-45

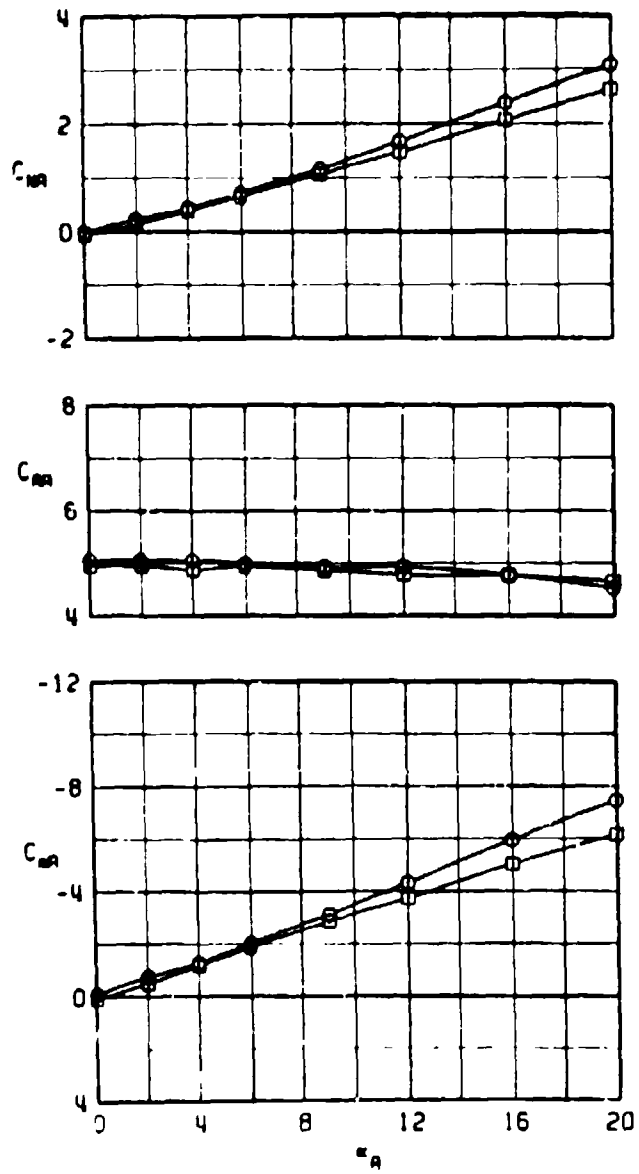

a. $M_\infty = 0.6$

Figure 9. Effects of model roll orientation on the static stability characteristics of the MK-84 with T2 fins, ϕ_B = -45 deg.

SYMBOL	M_∞	ϕ_M
○	0.6	0
□	0.6	-45

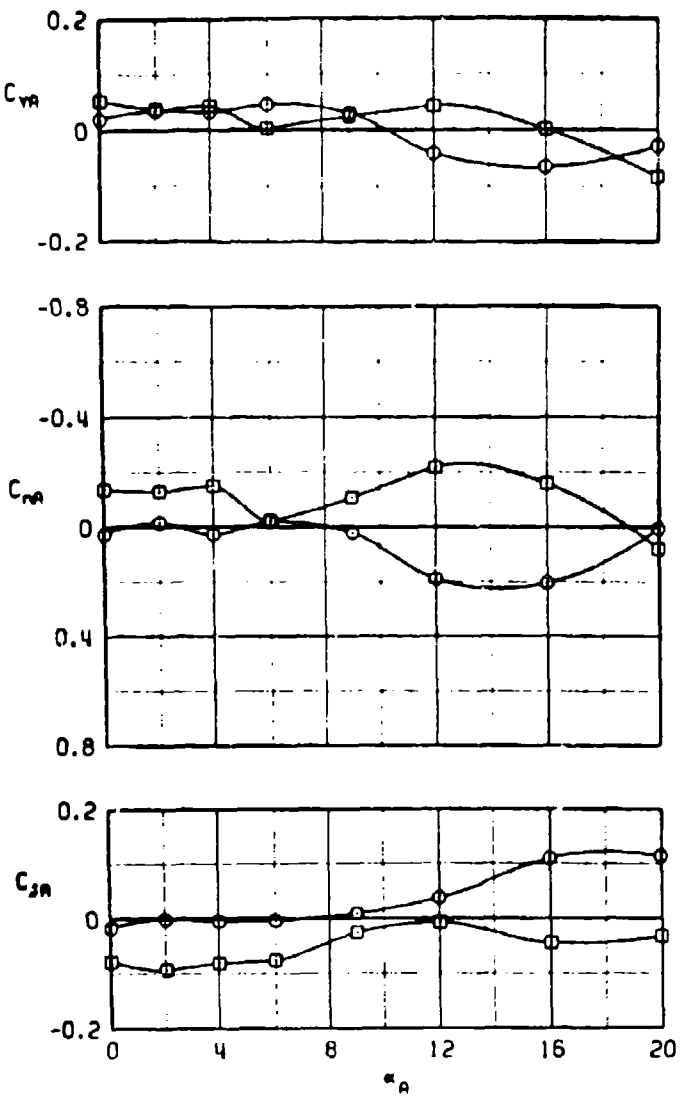

a. Concluded
Figure 9. Continued.

SYMBOL	M_∞	ϕ_p
○	0.8	0
□	0.8	-45

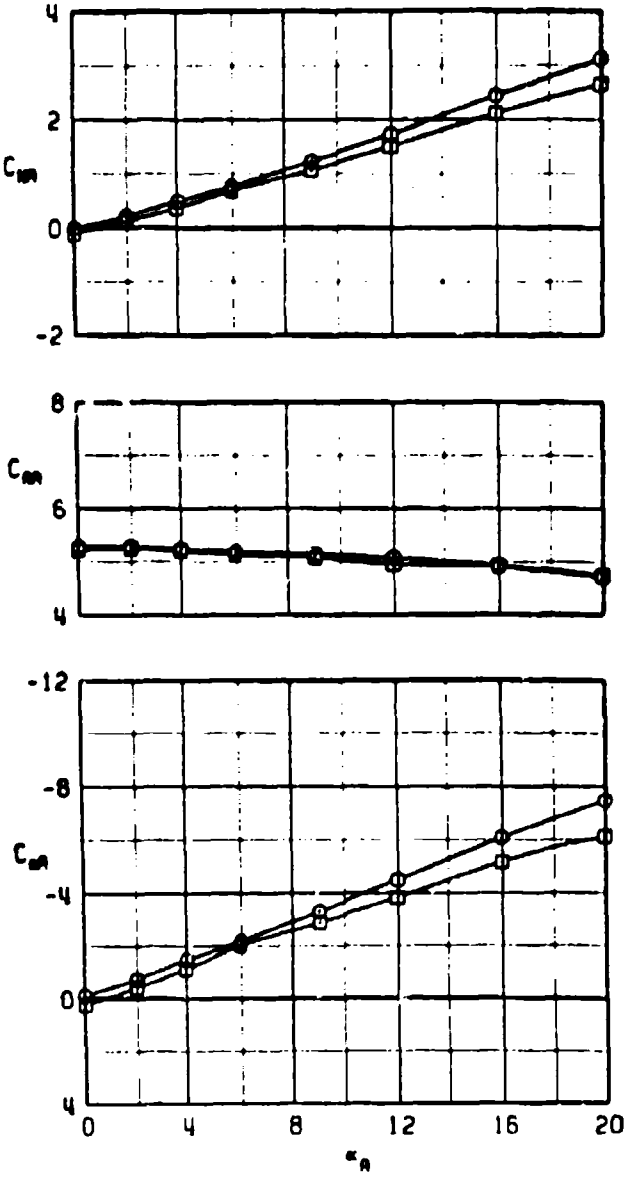

b. $M_\infty = 0.8$

Figure 9. Continued.

SYMBOL	M_∞	ϕ_w
⊙	0.8	0
⊡	0.8	-45

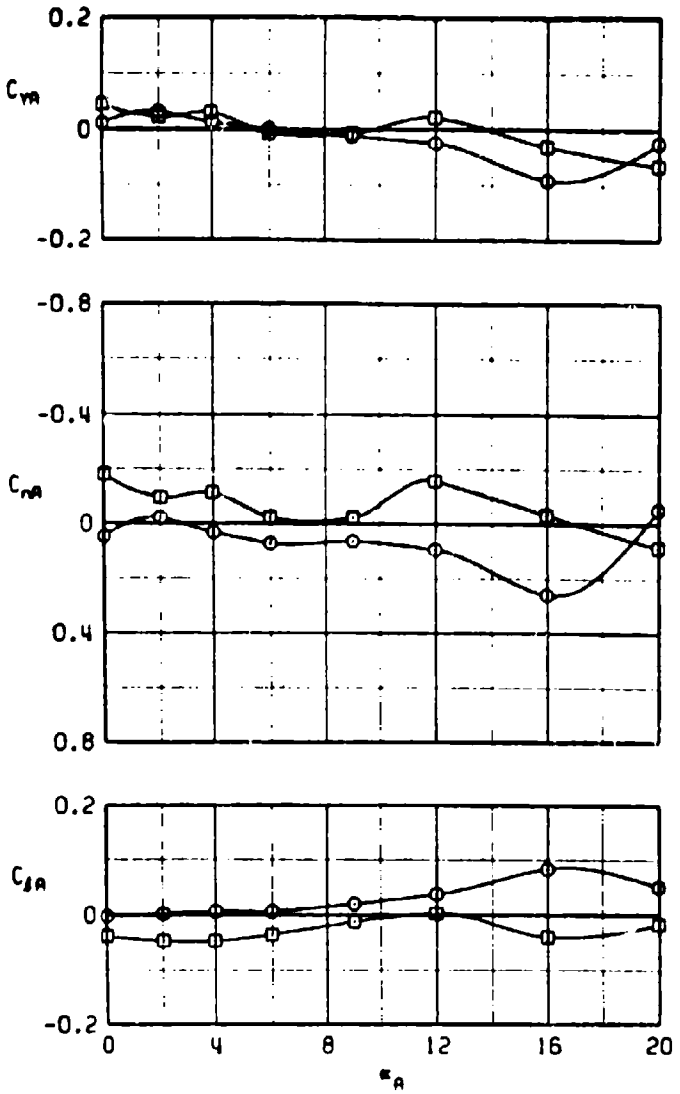

b. Concluded
Figure 9. Continued.

SYMBOL	M_∞	ϕ_w
⊙	0.9	0
⊡	0.9	-45

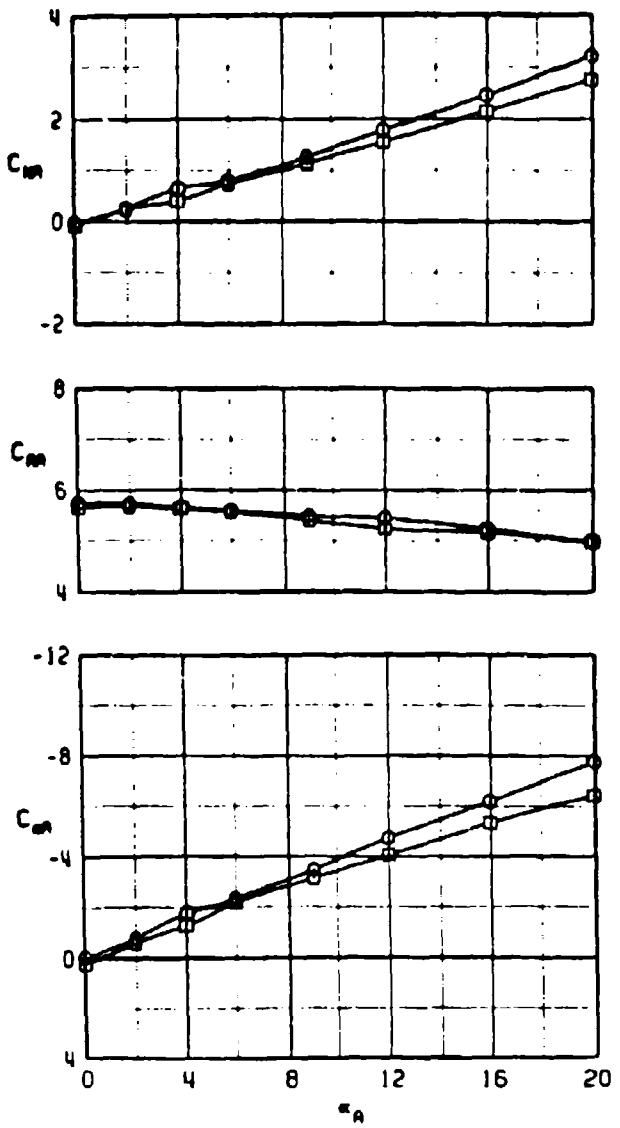

c. $M_\infty = 0.9$

Figure 9. Continued.

SYMBOL	M_∞	ϕ_R
○	0.9	0
□	0.9	-45

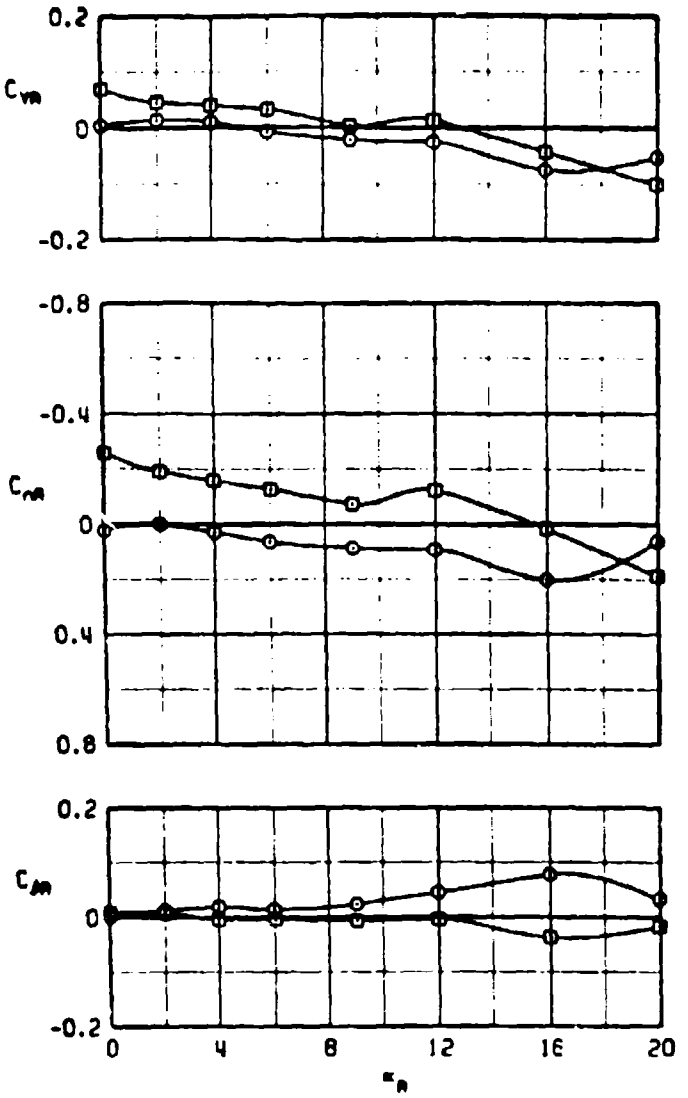

c. Concluded
Figure 9. Continued.

SYMBOL	M_∞	ϕ_m
⊡	1.0	-45

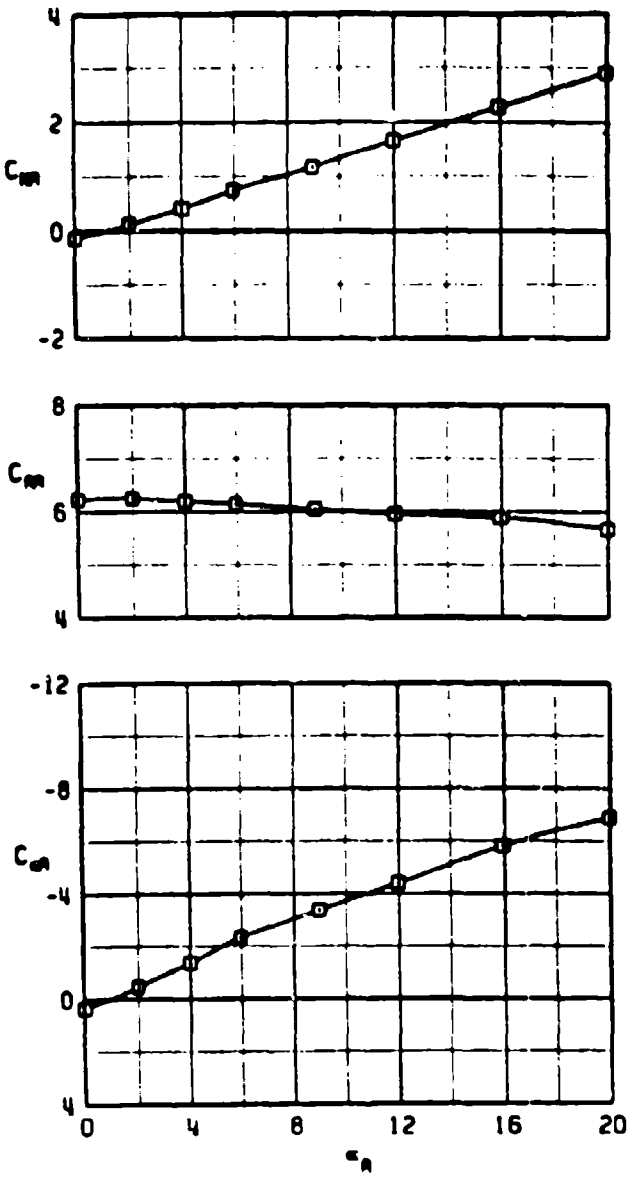

d. M_∞ = 1.0
Figure 9. Continued.

SYMBOL	M_∞	ϕ_w
⊡	1.0	-45

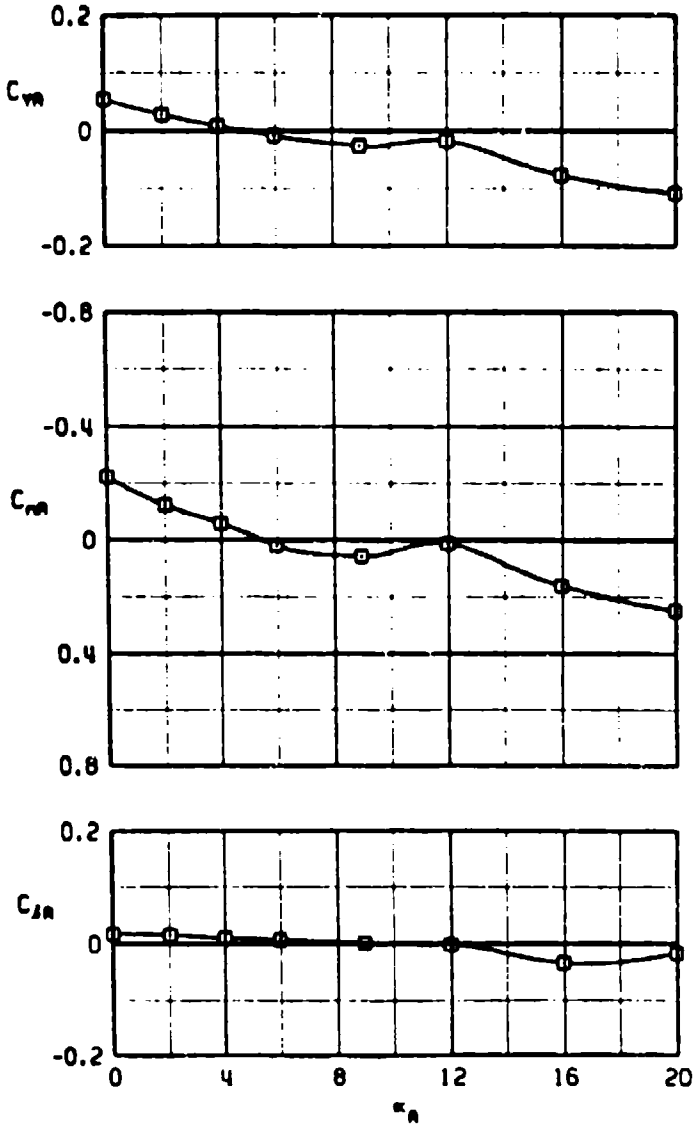

d. Concluded
Figure 9. Continued.

SYMBOL	M_∞	ϕ_B
⊙	1.1	0
⊡	1.1	-45

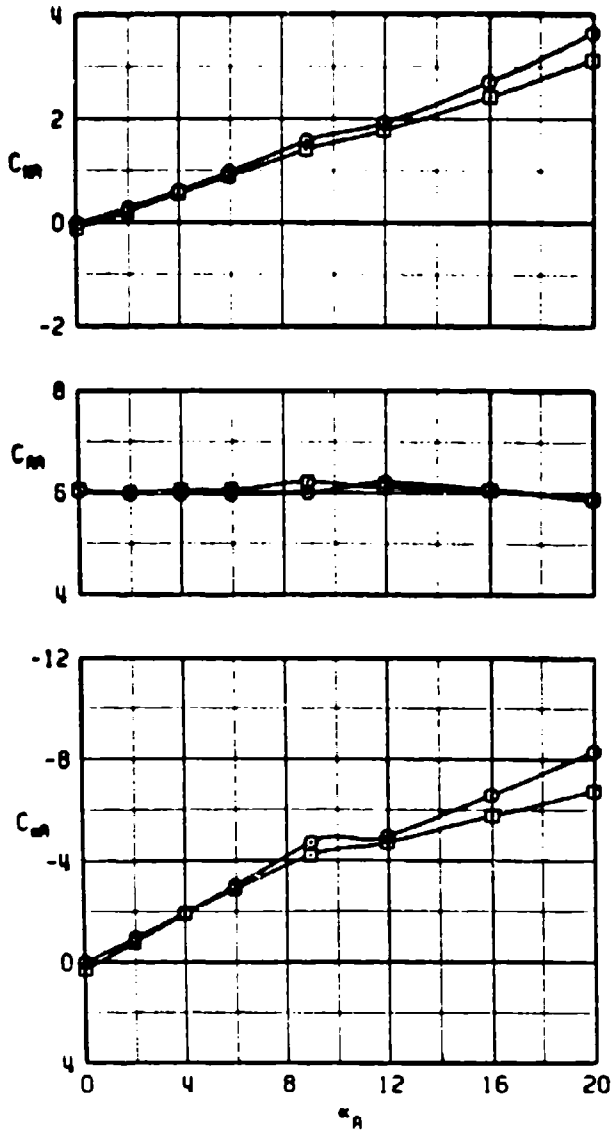

e. $M_\infty = 1.1$

Figure 9. Continued.

SYMBOL	M_∞	ϕ_w
⊙	1.1	0
⊡	1.1	-45

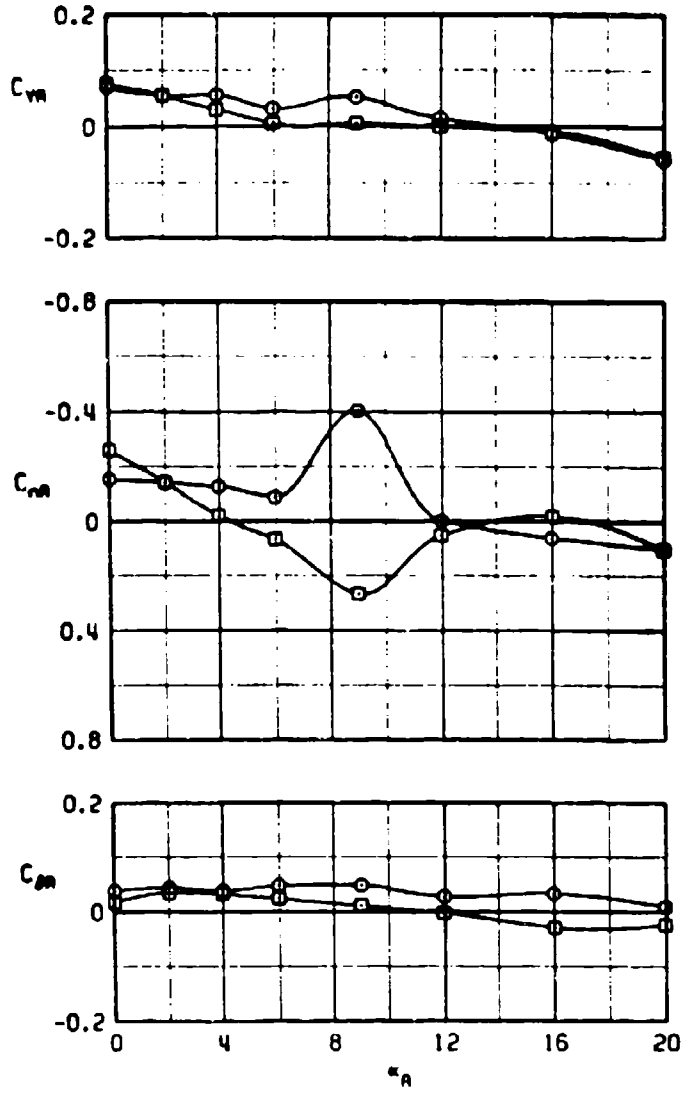

e. Concluded
Figure 9. Continued.

SYMBOL	M_∞	ϕ_R
⊡	1.2	-45

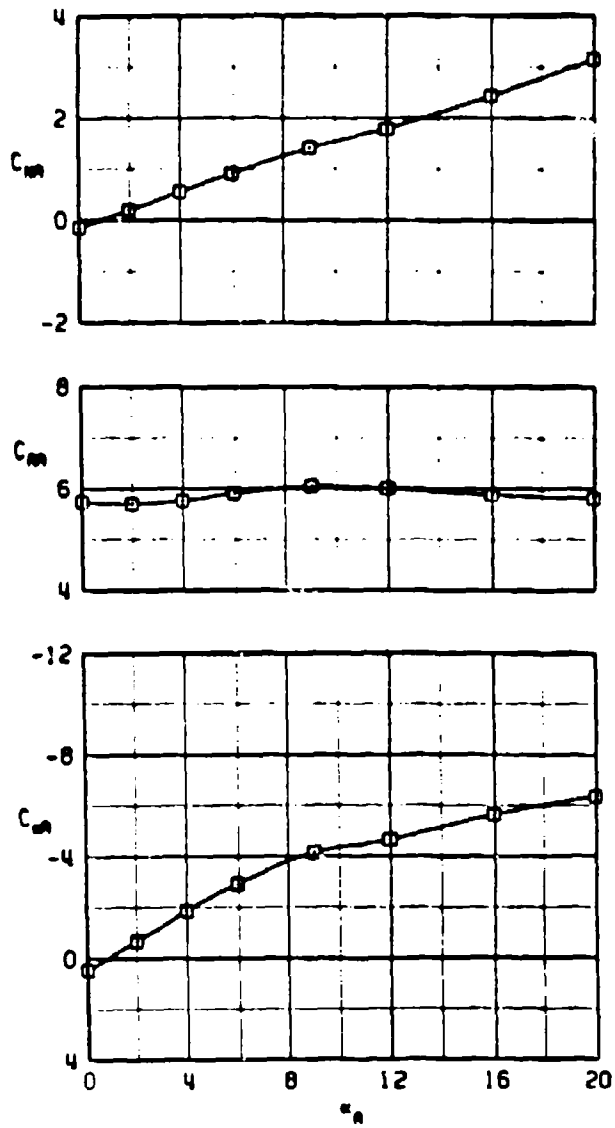

f. M_∞ = 1.2
Figure 9. Continued.

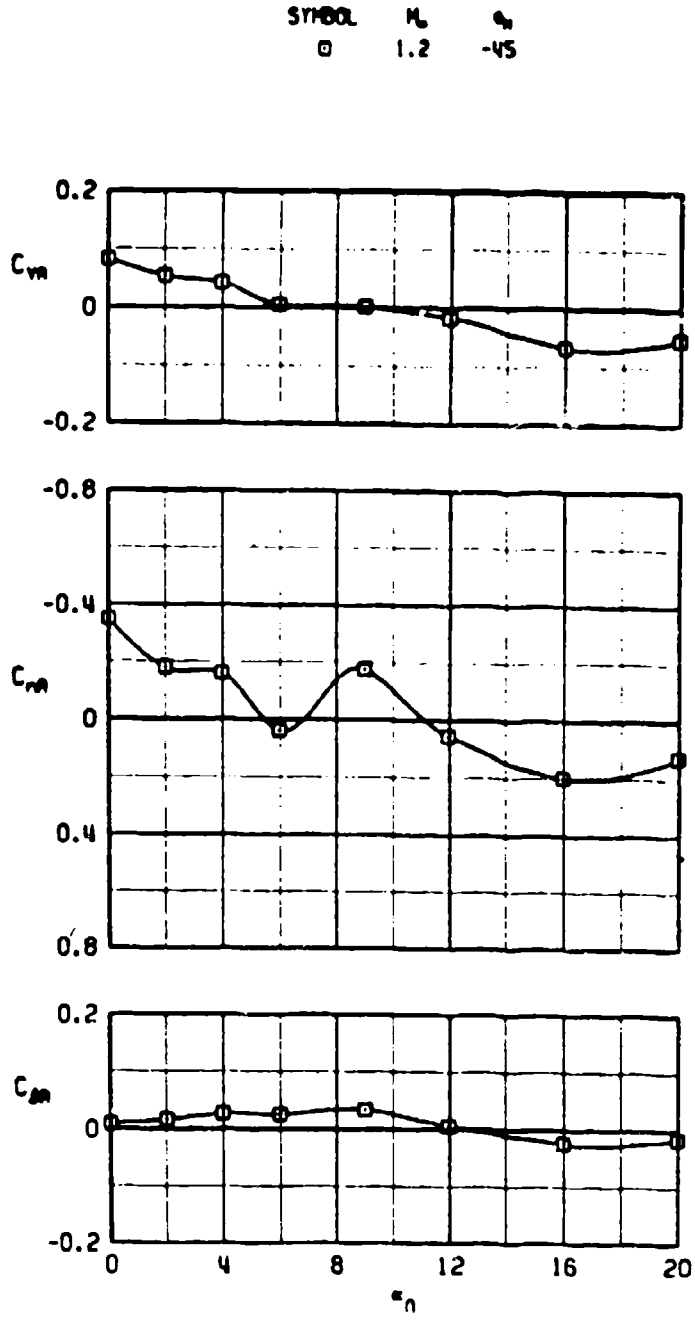

f. Concluded
Figure 9. Concluded.

SYMBOL	CONF	M_∞	ϕ_M
⊙	T2	0.6	-45
⊡	T3	0.6	-45

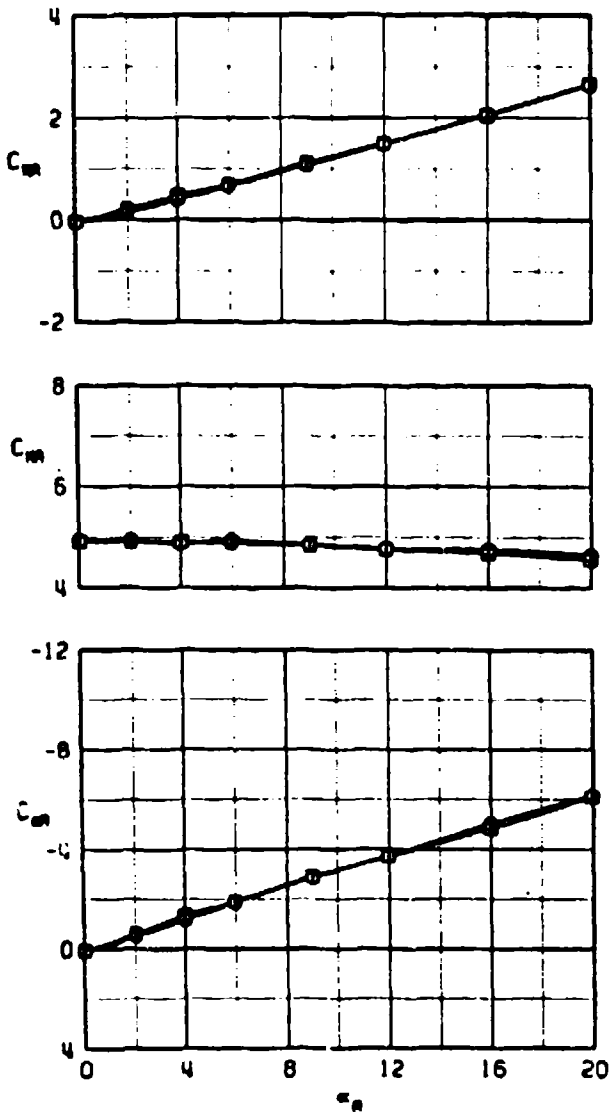

a. M_∞ = 0.6

Figure 10. Effects of fin configuration on the static stability characteristics of the MK-84, ϕ_B and ϕ_M = -45 deg.

SYMBOL	CONF	M_∞	ϕ_w
⊙	T2	0.6	-45
⊡	T3	0.6	-45

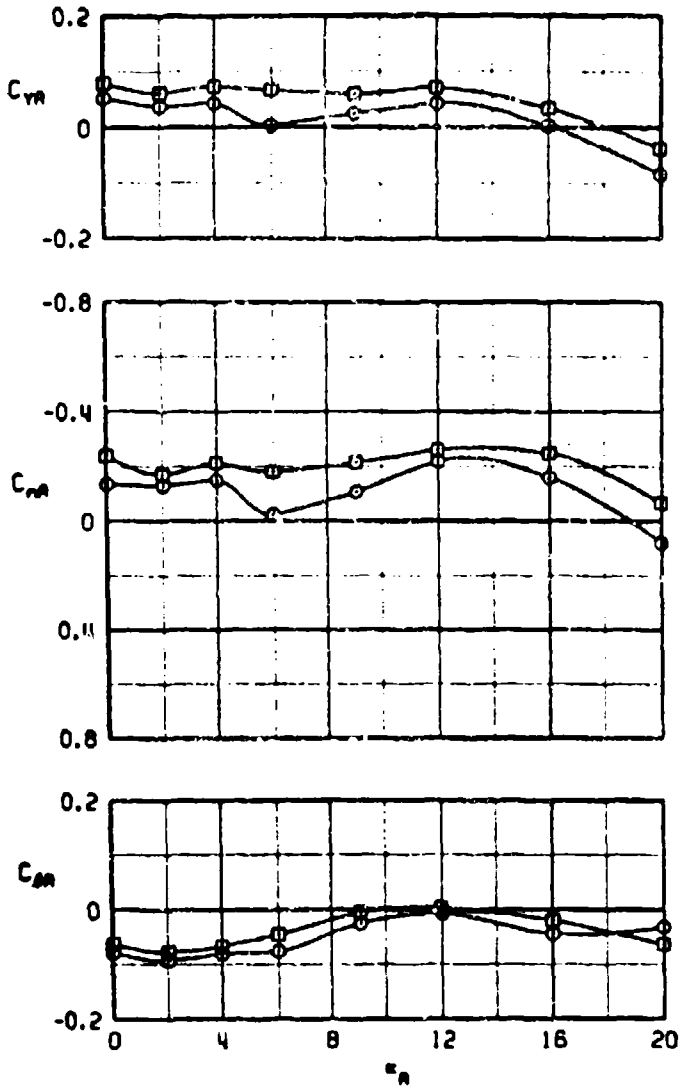

a. Concluded
Figure 10. Continued.

SYMBOL	CONF	M_∞	ϕ_R
○	T2	0.8	-45
⊡	T3	0.8	-45

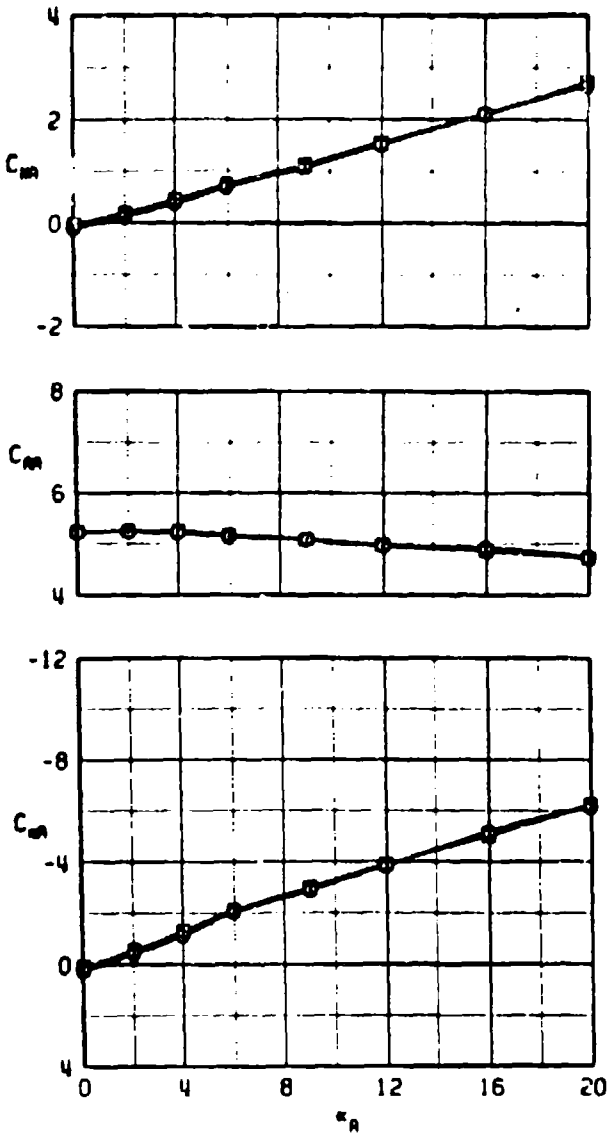

b. M_∞ = 0.8

Figure 10. Continued.

SYMBOL	CONF	M_∞	ϕ_n
⊙	T2	0.8	-45
⊡	T3	0.8	-45

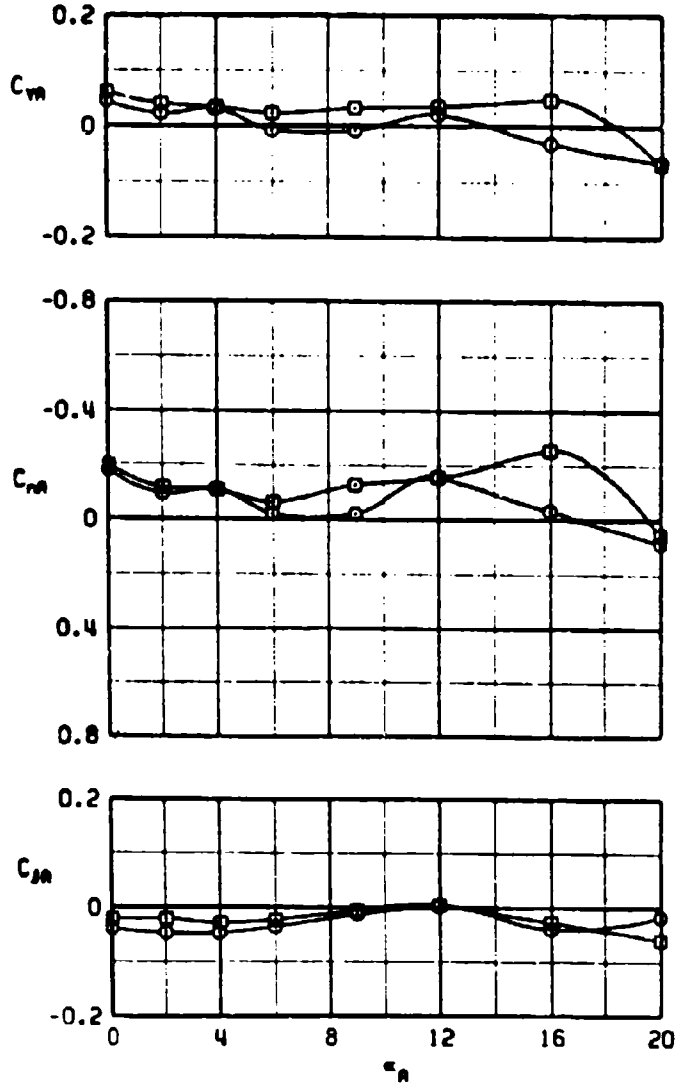

b. Concluded
Figure 10. Continued.

SYMBOL	CONF	M_∞	ϕ_w
⊙	T2	0.9	-45
⊡	T3	0.9	-45

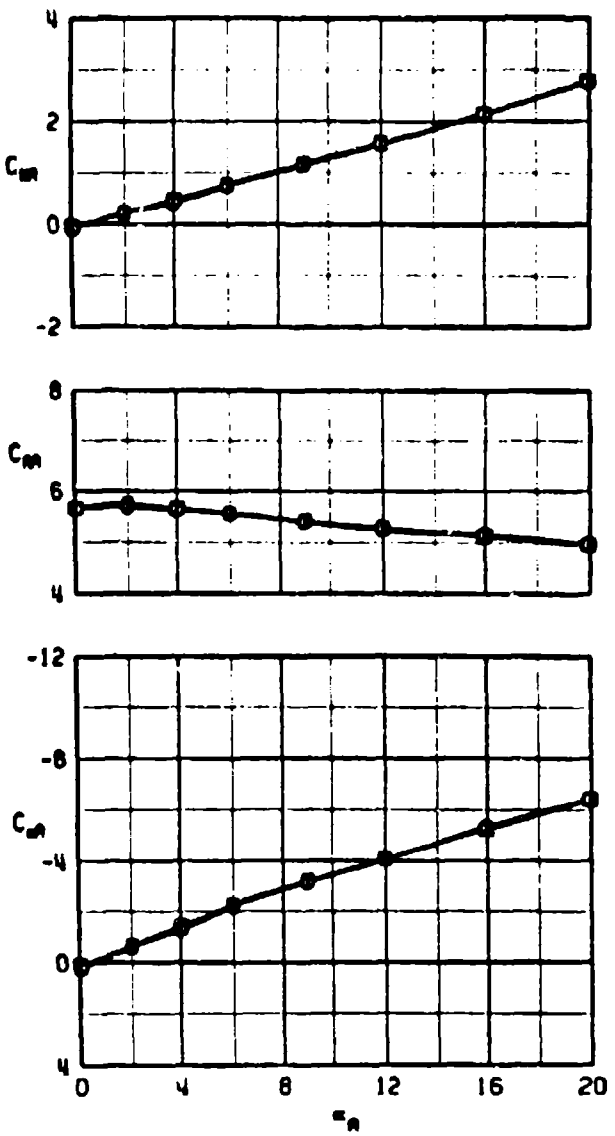

c. M_∞ = 0.9

Figure 10. Continued.

SYMBOL	CONF	M_∞	ϕ_w
○	T2	0.9	-45
□	T3	0.9	-45

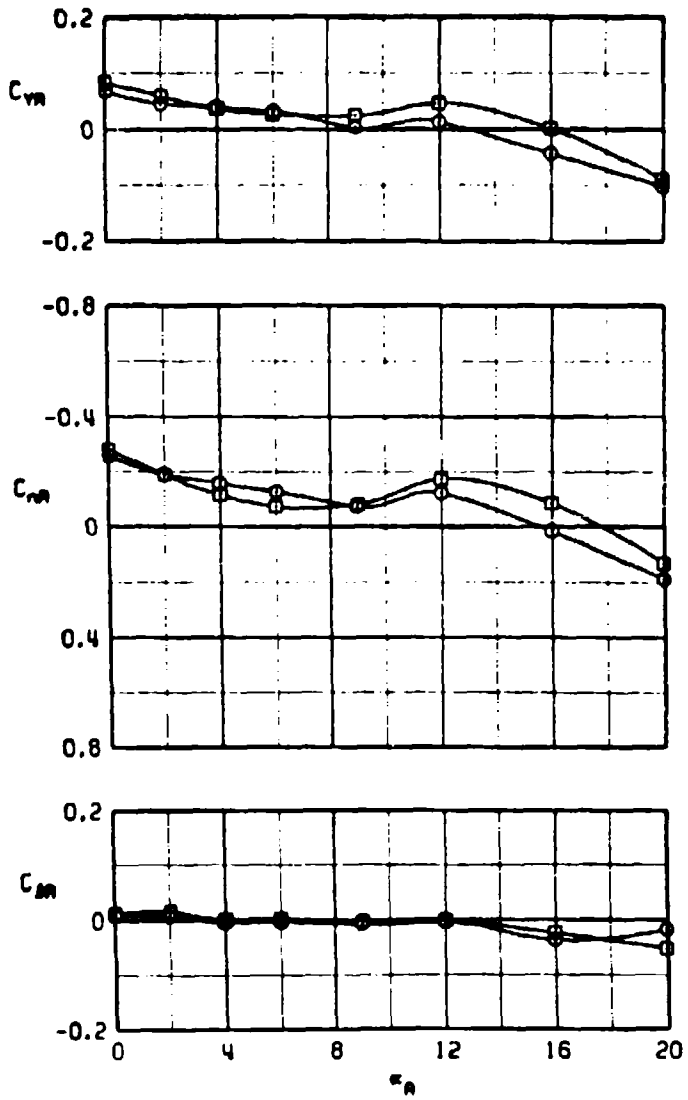

c. Concluded
Figure 10. Continued.

SYMBOL	CONF	M_∞	ϕ_n
⊙	T2	1.0	-45
⊡	T3	1.0	-45

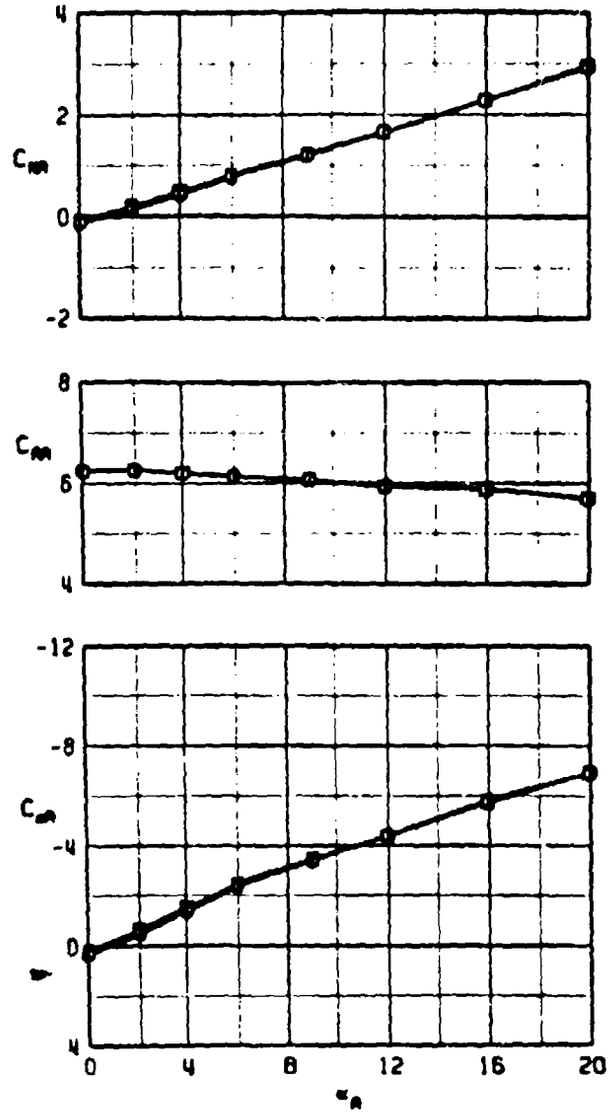

d. M_∞ = 1.0
Figure 10. Continued.

SYMBOL	CONF	M_∞	ϕ_w
○	T2	1.0	-45
□	T3	1.0	-45

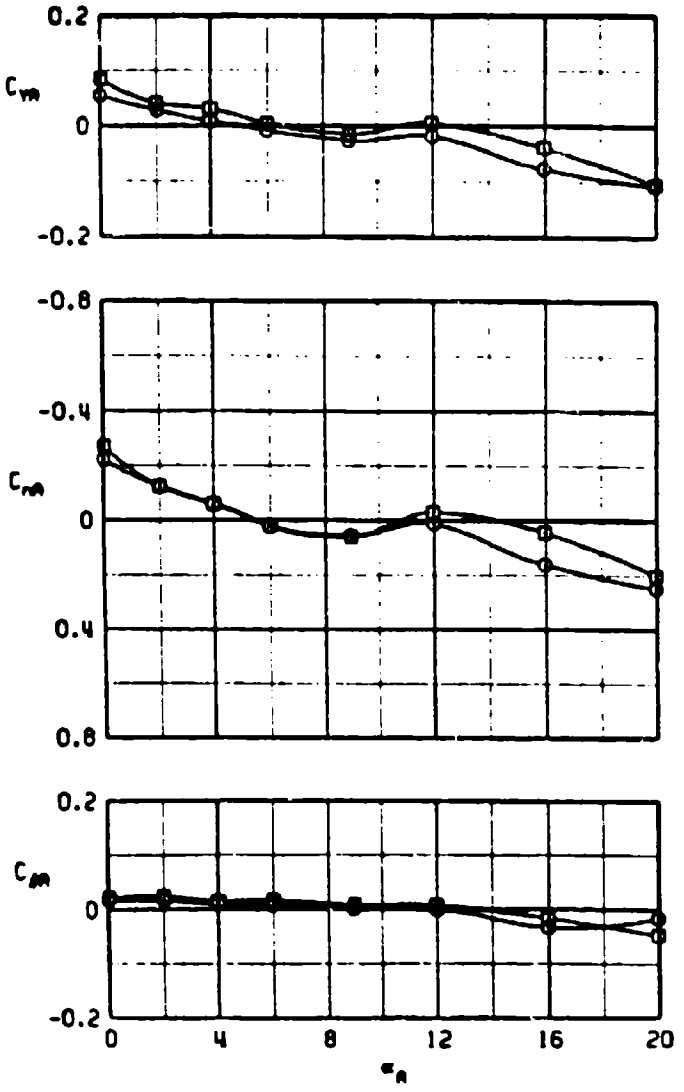

d. Concluded
Figure 10. Continued.

SYMBOL	CONF	M_∞	ϕ_w
⊙	T2	1.1	-45
⊡	T3	1.1	-45

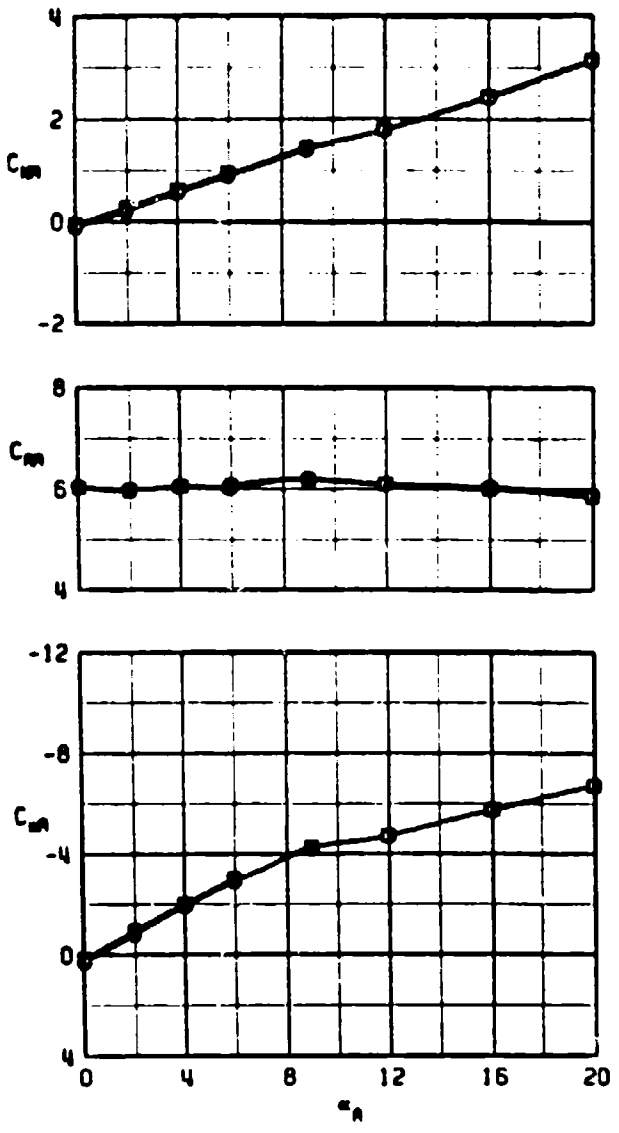

e. M_∞ = 1.1

Figure 10. Continued.

SYMBOL	CONF	M_∞	ϕ_w
⊙	T2	1.1	-45
⊡	T3	1.1	-45

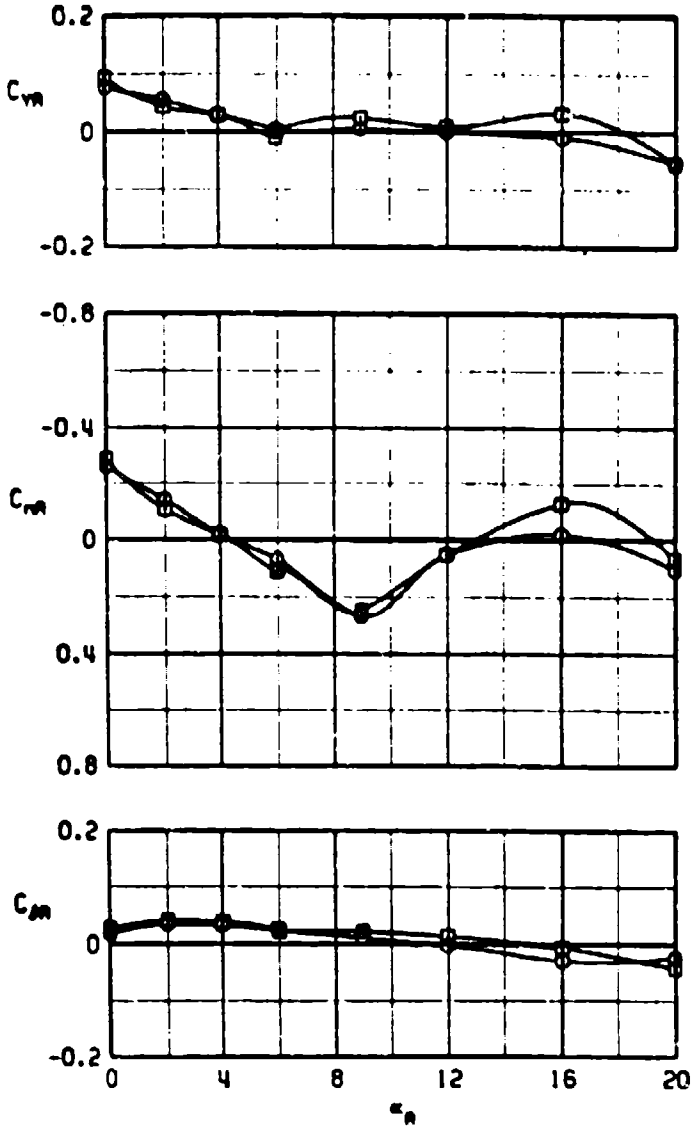

e. Concluded
Figure 10. Continued.

SYMBOL	CONF	M_∞	ϕ_R
⊙	T2	1.2	-45
⊡	T3	1.2	-45

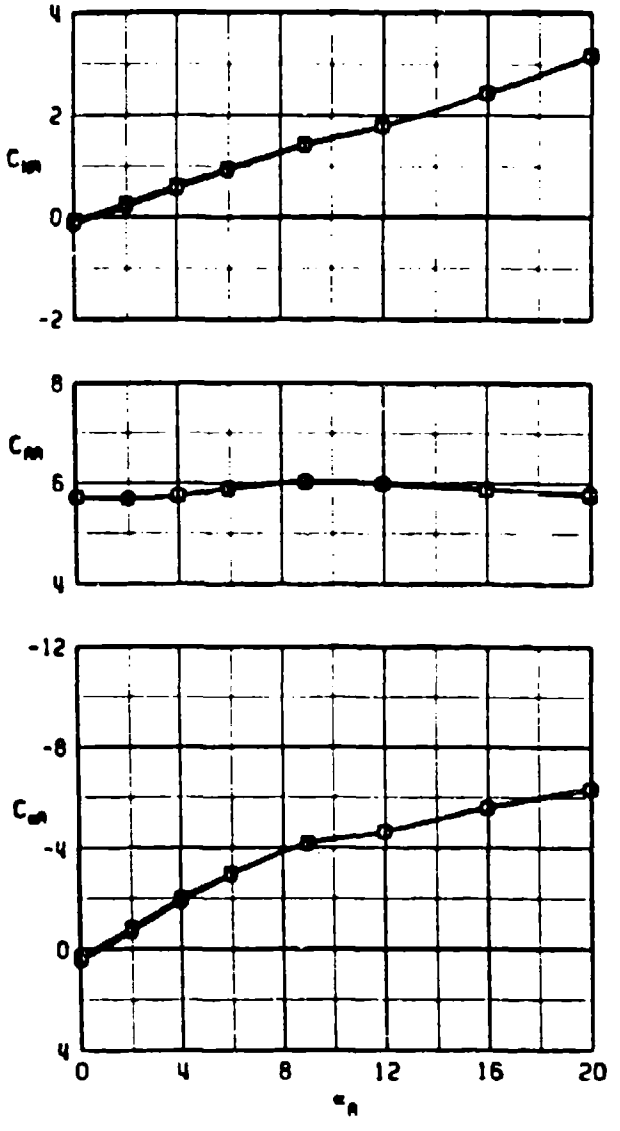

f. M_∞ = 1.2
Figure 10. Continued.

SYMBOL	CONF	M_∞	ϕ_R
⊙	T2	1.2	-45
⊡	T3	1.2	-45

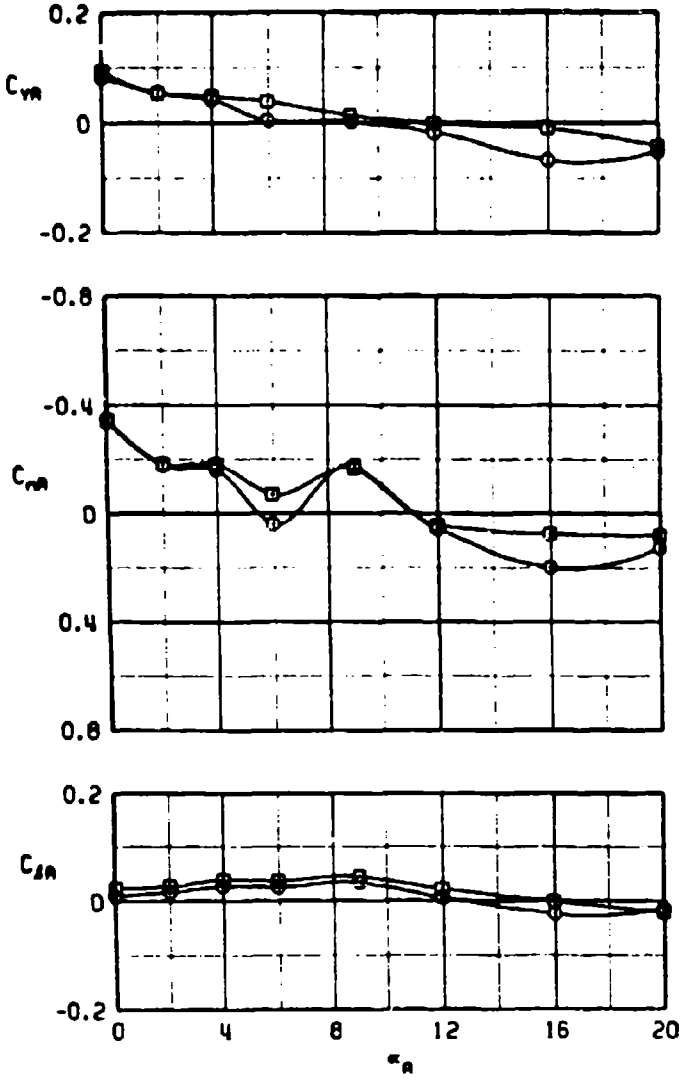

f. Concluded
Figure 10. Continued.

SYMBOL	CONF	M_∞	ϕ_m
⊡	13	1.4	-45

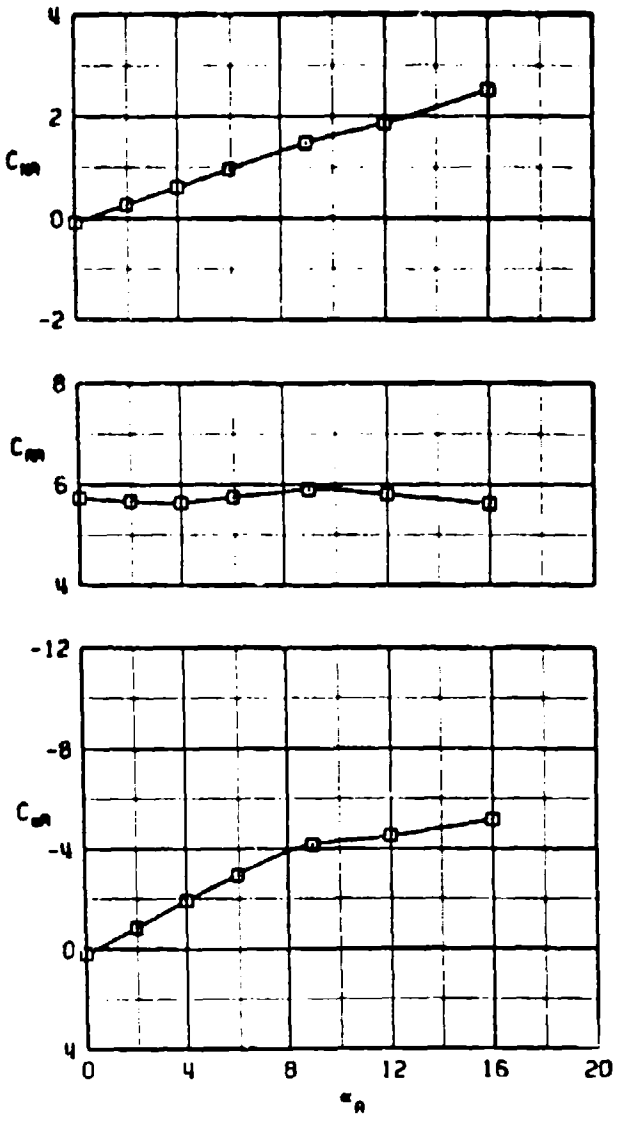

g. M_∞ = 1.4
Figure 10. Continued.

SYMBOL	CONF	M_∞	ϕ_m
⊡	T3	1.4	-45

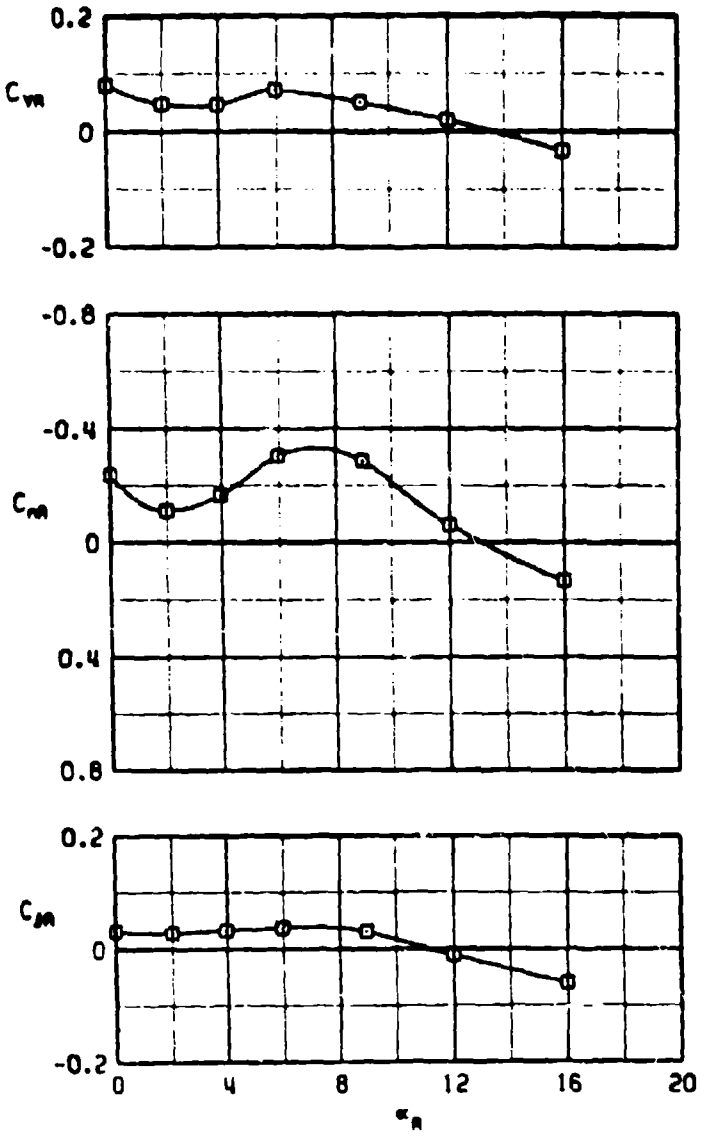

g. Concluded
Figure 10. Concluded.

NOMENCLATURE

C_{AA}	Axial-force coefficient, $F_A/q_\infty S$
$C_{\ell A}$	Rolling-moment coefficient, $M_\ell/q_\infty Sd$
C_{mA}	Pitching-moment coefficient, $M_m/q_\infty Sd$
C_{NA}	Normal-force coefficient, $F_N/q_\infty S$
C_{nA}	Yawing-moment coefficient, $M_n/q_\infty Sd$
C_{YA}	Side-force coefficient, $F_Y/q_\infty S$
d	Reference length, maximum diameter of model centerbody, 0.3958 ft
F_A	Measured axial force, lb
F_N	Measured normal force, lb
F_Y	Measured side force, lb
M_ℓ	Measured rolling moment, ft-lb
M_m	Measured pitching moment, ft-lb
M_n	Measured yawing moment, ft-lb
M_∞	Free-stream Mach number
MS	Model station
q_∞	Free-stream dynamic pressure, psf
Re	Reynolds number based on d
S	Reference area, 0.1231 ft^2
α_A	Model angle of attack, deg
ϕ_B	Ballute roll angle, deg
ϕ_M	Model roll angle, deg